Molecular Characterization of Comb Plates in the Ctenophore *Bolinopsis mikado*

January 2020

Kei JOKURA

Molecular Characterization of Comb Plates in the Ctenophore *Bolinopsis mikado*

A Dissertation Submitted to
the Graduate School of Life and Environmental Sciences,
the University of Tsukuba
in Partial Fulfillment of the Requirements
for the Degree of Doctor of Philosophy in Science
(Doctoral Program in Biological Sciences)

Kei JOKURA

Contents

Abbreviations

CBB	Coomassie Brilliant Blue
DAPI	4’,6-diamidino-2-phenylindole
DTT	dithiothreitol
EDTA	ethylenediaminetetraacetic acid
EGTA	ethylene glycol tetra-acetic acid
emPAI	exponentially modified protein abundance index
FSW	filtrated sea water
HEPES	4-(2-hydroxyethyl)-1-piperazineethanesulfonic acid
hpf	hours post-fertilization
IgG	Immunoglobulin G
KCl	potassium chloride
LC-MS/MS	liquid chromatography tandem-mass spectrometry
MALDI-TOF/MS	matrix-assisted laser desorption ionization-time of flight mass spectrometry
MOPS	3-(N-morpholino) propanesulfonic acid
PBS	phosphate buffered saline
PBST	0.05% Tween20 [polyoxyethylene (20) sorbitan monolaurate] containing PBS
PVDF	polyvinylidene difluoride
RT	room temperature
S.E.	standard error
SDS	sodium dodecyl sulfate
SDS-PAGE	SDS polyacrylamide gel electrophoresis
Tris	tris(hydroxymethyl)aminomethane

Chapter 1

General Introduction

1.1 The biology of cilia

The ciliary movement always makes us realize the dynamism of life. Since the first time when Gray observed the movement of cilia that grew up on the gills of the bivalve *Mytilus edulis* by high-speed photography (Gray, 1930), many researchers have been fascinated by the periodic movement for about 90 years. The ciliary movement consists of an effective stroke that produces a propulsive force and a recovery stroke that returns with a small resistance. In the effective stroke, a remarkable bend occurs locally in the part near the root and the entire most part is kept almost straight during the inclination changes. In the recovery stroke, an opposite bend is generated at the base and propagates along the cilium. Such an asymmetric waveform is generally called the "ciliary" movement (Fig. 1.1A). The movements are very diverse among organisms, organs and tissues, in terms of beat frequency and the planarity of a wave. However, the internal cytoskeletal structures of cilia, called the axonemes, are widely common and have been conserved with almost no change from protists to human in the long evolutionary history.

The axoneme is composed of nine doublet microtubules and two central pair microtubules (9+2 structure) (Fig. 1.1B). The axonemal dyneins are molecular motors that move on a doublet microtubule, creating its bending for ciliary movement. In addition, the ciliary movement is regulated by the interactions among approximately 250 proteins (Nakachi et al., 2011). The structure and function of the axoneme have been studied genetically, physiologically, and biochemically for decades. Recently, the study of cilia has been greatly developed by the advances in structural biology and genetic engineering. However, much remains unknown about the mechanism of ciliary movement.

When multiple cilia are aligned in rows or planes, each cilium has a hydrodynamic interaction with neighboring cilia and beats in a way that maintains a phase difference. As a result, a large wave, called metachronal wave, is formed across the aligned cilia (Sleigh, 1962). According to a modeling and simulation, the metachronal wave increases the propulsion velocity to more than 3-fold and the efficiency almost to 10-fold compared with cilia beating all in a phase (Elgeti and Gompper, 2013). The directions of the effective stroke and the metachronal wave are kept coincident. When cilia are arranged in parallel with the direction of ciliary movement, the direction of metachronal rhythm is divided into two types. One type is the transmission of the rhythm to the direction of effective stroke (symplectic), and the other is to the direction of recovery stroke (antiplectic) (Knight-Jones, 1954) (Fig. 1.1C). In the symplectic metachronism, cilia are put together at the time of the effective stroke. Therefore, this type is thought to be suitable for sending highly viscous liquids or particles with a large

force. In contrast, the antiplectic metachronism is thought to be suitable for quickly sending low viscosity liquids, because the distance between the cilia becomes longer during of effective stroke. Recent studies have reported that the fluid-mediated hydrodynamic interactions between neighboring cilia are the important feedbacks for coordination of ciliary movement (Mitchell et al., 2007). The flow formed by the ciliary metachronal wave is critical not only for the swimming of living organisms but also for several important biological processes, such as gamete transport, removal of waste products, and transport of signaling molecules.

The antiplectic metachronal waves are known in several organisms, such as antero-dorsal cilia of the planarians, lateral frontal cilia in the gills of bivalves, the collar and trunk cilia of acorn worms and the comb plates of ctenophores (Knight-Jones, 1954). The comb plate composed of bundled cilia, called compound cilia, and provides a good model for understanding the hydrodynamic principle of antiplectically coordinated paddles. The compound cilia are known in cirri of the *Euprotes*, membranelle and lateral frontal cilia in the gills of bivalves. Reynolds number has been used for a long time for the hydrodynamic understanding of ciliary movement. The Reynolds number of a motile system determines the flow in an aquatic solution. It is affected by the length and angular velocity of a substance. If it is less than 1, such as the case with low velocity or smaller size, the viscous forces become dominant; whereas if the value is more than 1, inertial forces dominates the viscous forces. Many cilia are several tens of micrometers in length, and their movement is dominated by viscous forces. However, some compound cilia including the comb plates are longer than general cilia, and thus the inertial force cannot be ignored. In the case of comb plates, the Reynolds number is estimated to be close to 10 because its length is 1 mm or more (Barlow et al., 1993). This means that the inertial force acts 10 times the viscous force. The antiplectic metachronal wave generated by the comb plates is considered to be an example for efficiently functioning cilia that are affected by inertial force (Barlow and Sleigh, 1993).

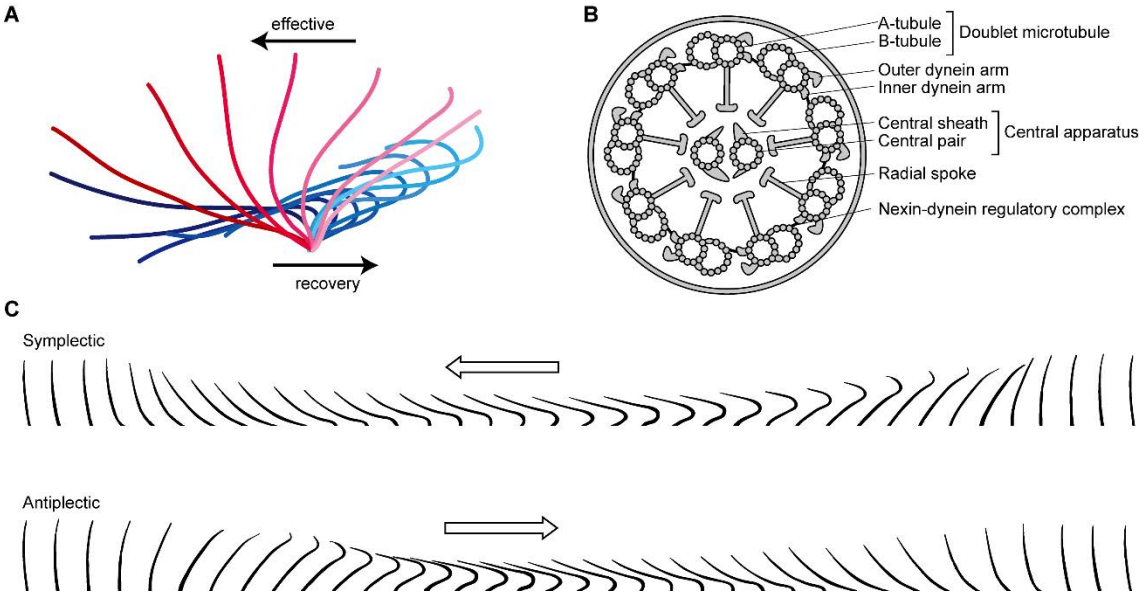

Fig 1.1. Structure and movement of cilia

(A) One cycle of typical ciliary movement. Red lines are effective strokes and blue lines are recovery strokes. (B) A schematic diagram of a cross-sectioned cilium. (C) Schematic diagram of two types of metachronal waves. Effective stroke direction is right to left. Arrows indicate the direction of wave propagation. Top, symplectic type. The directions of effective stroke and wave propagation are the same. Bottom, antitiplectic type. The directions of effective stroke and wave propagation are opposite.

1.2 Ctenophores

Ctenophores, or comb jellies, are gelatinous marine invertebrates that distribute worldwide. Approximately 100 to 150 species of ctenophores are described to date. Despite the gelatinous bodies, ctenophores have fossil records from early Cambrian period, about 540 million years ago (e.g. Zhao et al., 2019). The phylum Ctenophora is grouped in the animals with simple body plans called basal metazoans, together with Cnidaria, Placozoa and Porifera. Recent advances in the genome projects positioned the Ctenophora to the first group of animals that appeared after multicellularization (Fig. 1.2.; Ryan et al., 2013). In fact, Ctenophores lack key homologs for a set of genes that are involved in body patterning and development crucial in Cnidaria and Bilateria, including homeobox genes of the Hox and ParaHox classes (Ryan et al., 2013) and the genes for major components of the Notch and Hedgehog cell signaling pathways (Moroz et al., 2014; Ryan et al., 2013). In addition, they have no Hox gene for neuronal segmentation and few genes for classical neurotransmitters found in other animals. However, ctenophores have clear and sophisticated nerve systems, although either Porifera or Placozoa does not. It is often discussed that the appearance of the nervous system occurred independently in Ctenophora and Cnidaria and that the acquirement of nerve system in Ctenophora is the result of convergent evolution (Moroz et al., 2014). Thus, either the phylogenetic position or the evolutionary process of Ctenophora is very mysterious and still remains controversial.

The extant species of ctenophores are conventionally classified into six orders, although a systematic classification has not yet been established and several orders still show multi-lineage (Fig. 1.3). Cydippida has commonly spherical body forms and long tentacles. The species in the order are recently proposed to be separated into four new orders, among which the Euplokamididae is thought to be the first emerged group of Ctenophora (Granhag et al., 2012; Simion et al., 2015). Lobata has a large lobe around its mouth. The species *Bolinopsis mikado* used in this study and the widely studied species *Mnemiopsis leidyi* are included in this order. Beroida has no tentacles in the whole life cycle. This group of ctenophores has a huge mouth equipped with countless teeth, “macrocilia” and eats other species of comb jellies. Other three orders of Ctenophore show unique morphologies. Cestida, represented by a well-known “Venus girdle”, has a flat and elongated body, with the length reaching 2 meters at the maximum. Platyctenida is primarily benthic. The body is flattened, creeping on a substratum. The comb plates degenerate during metamorphosis in all but one species. Thalassocalycida represents an umbrella-like shape that is unusual for ctenophores. It has a single species, *Thalassocalyce inconstans*.

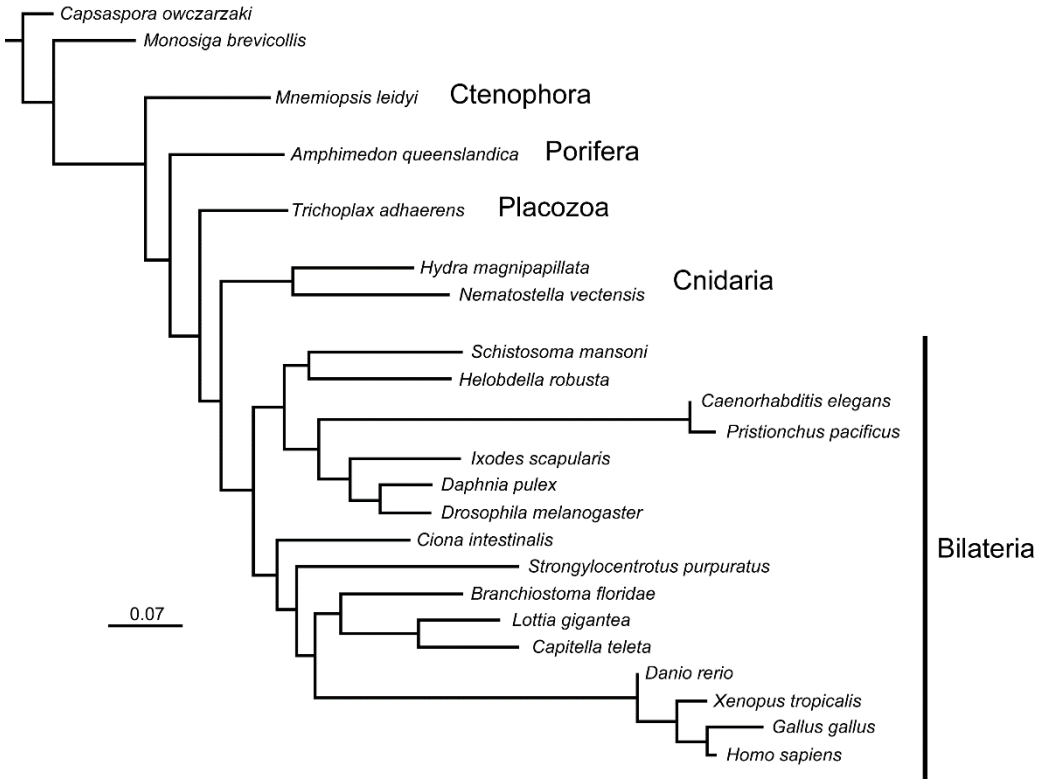

Figure 1.2. Animal phyla tree produced by maximum-likelihood analysis of gene content
Modified from Ryan et al., 2013.

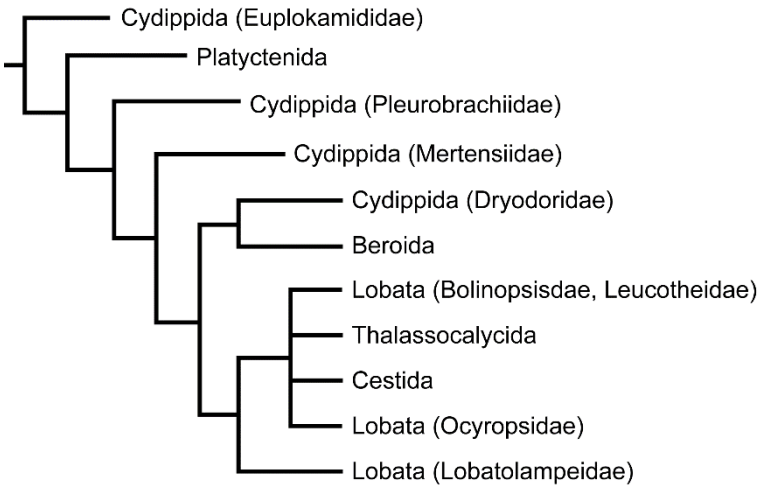

Figure 1.3. Evolutionary relationships in Ctenophora
The Cydippida and Lobata are multilineages. *Bolinopsis mikado* used in this study and *Mnemiopsis leidyi* whose genome is published are classified as Bolinopsisdae in Lobata. Modified from Whelan et al., 2017.

Cnidarians and ctenophores were once grouped into the same phylum Coelenterata because they have several similarities in common, such as gelatinous material called mesoglea and the network of nerve cells called nerve net. Ctenophore, however, have relatively a sophisticated nervous system that is composed of a peripheral polygonal nerve net, apical organ, and tentacular nerves (Hernandez-Nicaise, 1973; Horridge, 1974; Martindale and Henry, 1997; Tamm, 1982). In addition, Ctenophores have no cnidocytes, one of the characteristics in cnidarians, but have sticky cells called colloblasts (Franc, 1978; Weill, 1935). In cnidarians, bioluminescence is often used for communication between individuals. More recently, the first photoproteins from ctenophores have also been cloned and found to be localized along the base of comb rows (Markova et al., 2012). It has been reported that chemical or optical communication between pairs is important for successful gamete trading (Sasson et al., 2018).

One of the most notable characteristics of Ctenophores is the iridescent eight comb plates rows to facilitate their locomotion. They are the largest animals to swim with the help of ciliary movement. The eight comb rows are arranged radially at a glance, therefore they tend to be considered to have radial symmetry. However, they consist of four quadrants with two comb rows, separated by two planes (tentacle and sagittal plane). Adjacent quadrants are similar but not morphologically identical because two opposite quadrants have anal pores (Martindale and Henry, 1995; Tamm, 2019) (Fig. 1.4). Thus, they have an infinite number of planes of rotational symmetry.

Almost all ctenophore species are hermaphroditic and undergo external fertilization. The fertilized eggs of ctenophores are famous as “mosaic” eggs in which the fate of each blastomere is determined very early in the development, thus, ctenophore embryos have played an important role in the study of developmental mechanism in the history of developmental biology (Chun, 1880; Driesch and Morgan, 1895; Martindale, 1986). Most, but not all ctenophores are self-fertile hermaphrodites. Male and female gonads are associated with the sub-comb row canal in the endodermal canal system. Spawning is generally triggered by the changes in photoperiod. In most cases, spawned oocytes have already undergone first and second polar body formation and have a surrounding acellular vitelline membrane made by the oocytes (Martindale and Henry, 2015). Ctenophore eggs and embryos are relatively large, not so difficult to be handled by manipulation. The comb plates start to grow out at the same time when as to the dome and balancer cilia begin associated with apical organ. By 14-16 hpf at 20°C, the ctenophore body plan becomes clear and the swelling of the mesoglea gives rise to an almost perfectly clear and spherical cydippid-stage animal. Then the motile comb plate cilia continue

to form, orient into individual plates and begin to beat in coordinated fashion. Each of the four subtentaclar comb rows has six comb plates, whereas each of the four subsagittal rows has five comb plates. This number does not change until hatching. The final step before hatching is the growth of the tentacles out past the body wall at approximately 24 hpf.

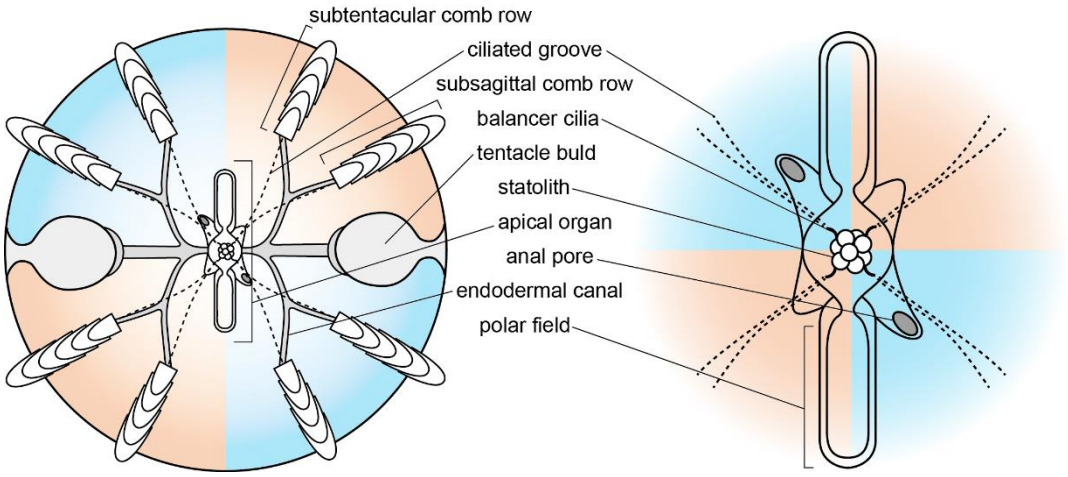

Figure 1.4. Diagrammatic illustration of the ctenophore body plan (aboral view).
Oranges and blues represent the same quadrants. There are anal pores in the blue quadrants. The axis of two the tentacle bulbs defines the tentacle planes, and the perpendicular one is termed sagittal planes. (Left) The ctenophore larva just after hatching. In each quadrant, there is a subtentacular comb row with 5 comb plates and a subsagittal comb row with 6 comb plates. (Right) An enlarged view of apical organ. Blue two opposite quadrants have anal pore. Modified from Martindale and Henry, 1995.

1.3 The hidden biology of ctenophores

From a phylogenomic analysis, Dunn et al. (2008) reported a strong support for the placement of ctenophores, rather than sponges, as the sister group to all other animals. However, ctenophores have many unique morphological features, which are not shared with other animals. Therefore, they gave little insight into how ctenophores are related to other animals. The unique features of ctenophores that has yet to be elucidated are “hidden biology”, which has been attracting attention of biologists as and is to be studied at the molecular and cellular levels (Dunn et al., 2015; Leys, 2019). For example, they lack miRNA and miRNA-processing machinery (Maxwell et al., 2012). The ctenophore nervous system is unique (Jager et al., 2011), with interconnected nerve nets (not just excitable epithelia) with synapses, but it lacks many of the neurotransmitters found in Bilateria. Moreover, ctenophores have giant smooth muscle cells (multinucleate and 4-cm long) (Martindale and Henry, 1999) and some have striated muscle (Mackie et al., 1988). The giant compound cilia, the comb plates, are also one of the hidden biology of ctenophores. The comb plate is a bundle of tens of thousands of very long cilia and generates strong flows efficiently without breaking up (Tamm, 1973). More studies on the molecular structures and functions of these systems should shed light on the biology of this unrelated family that are otherwise uncatalogued.

1.4 The compound cilia of the ctenophores

One of the pioneer scientists for ctenophore biology, Sidney Tamm, once said, “Truly, cilia and ctenophores, like love and marriage, go together like a horse and carriage” (Tamm, 2014). Ctenophores have evolved various unique compound cilia. The most distinctive feature of ctenophore molticilia is the **comb plate**. The “*cteno*” mean a “comb” in Greek, for which the ctenophores or the comb jellies were termed. Eight lines in most ctenophore body where the comb plates are aligned are called comb rows. The ctenophores perform swimming and posture control using the movement of the comb rows. The movement of the comb rows is controlled by the gravity sensor “apical organ” located on the aboral center of the ctenophores.

Four compound cilia, each composed of 50-200 motile mechanoresponsive cilia in the apical organ, are called **balancer cilia**, which support a large statolith in the center. The ciliary movements of the four balancer cilia change in response to the orientation of the statolith. A narrow furrow covered with short cilia, called a ciliated groove, is connected to each the balancer and is branched into two ways. The eight furrows are connected to the first comb plate in each comb row in the closest area of the apical organ. The ciliary movements of the balancer cilia propagate to subsequent two comb rows through the ciliated grooves. In other words, the ciliary movements of each of the four balancer cilia at the apical organ govern the initiation of metachronal waves of comb rows via ciliated grooves.

Beroe has countless compound cilia called **macrocilia** in their mouth. A single macrocilium is typically 25-30 μm long and 5 μm in diameter and consists of several hundred cross-linked 9+2 axonemes surrounded by a common membrane (Horridge, 1965; Tamm and Tamm, 1985; Tamm and Tamm, 1988). Adjacent axonemes are connected by link structures extending from 3 and 8 doublet microtubules. The orientations of axonemes are aligned, so that all the axonemes beat in synchronization. The macrocilia also have effective and recovery strokes as well as normal ciliary movement and form huge metachronal waves. When *Beroe* finds another ctenophore, *i.e.* the prey, it opens the mouth wide and wraps around the ctenophore in just 0.25 seconds. Then *Beroe* drags the prey into the stomach using the powerful metachronal waves of macrocilia (Tamm, 1983).

The structures and the movements of ctenophore compound cilia have been studied since 1950’, mostly in the comb plates. The metachronal waves of the comb row show antiplectic metachronism. The fluid flow around the ctenophore body is caused by the antiplectic waves toward the apical organ, therefore the ctenophores swim with the mouth side forward. Among ctenophore families, *Beroe* have the highest swimming ability using the comb plates and can search for other ctenophores while

swimming. The cydippid *Pleurobrachia pileus* uses the water flow for the force to spin the body to capture prey by the long tentacles into the mouth (Tamm and Moss, 1985). In the lobate *Mnemiopsis leidyi*, the antiplectic waves by the comb plates produce week water flows, so that it slowly accesses to the prey, such as copepods. They catch prey by enclosing with large lobes and transport it to the mouth (Colin et al., 2010).

Chapter 2

Biochemical characterization and functional analysis of CTENO64

2.1 Introduction

Comb plates are iridescent motile organs that characterize ctenophores (Fig. 2.1A). They are giant compound cilia that consist of tens of thousands of cilia with lengths up to 1 mm (Afzelius, 1961; Horridge, 1964; Tamm and Tamm, 1981) (Fig. 2.1B). All the cilia in a comb plate are arranged to be aligned with the same axonemal orientations. Each cilium has connected each other by structures called compartmenting lamellae (CL), which extend from two doublet microtubules (number 3 and 8) of the ciliary axonemes toward the plasma membrane (Afzelius, 1961) (Fig. 2.1C). Dentler (1981) found that the compartmenting lamellae of adjacent cilia are connected by filamentous interciliary bridges, which extend through the ciliary membranes and bind adjacent cilia together (Fig. 2.1D). The CL are thought to be important for the proper orientations and the mechanical synchronous movement of comb plate cilia. Since the comb plates have fine periodic structures, the light reflected from the comb plates interferes with each other and produces a rainbow structural color (Welch et al., 2005). However, the molecular structures and formation mechanism of the comb plates have not been completely elucidated. In particular, no component of CL has been identified, and the functions of CL are not known at all. In this chapter, I first describe the method for rearing ctenophores and isolating the CL that I have established during my study and then report the function of a protein CTENO64 that is specifically localized in the CL.

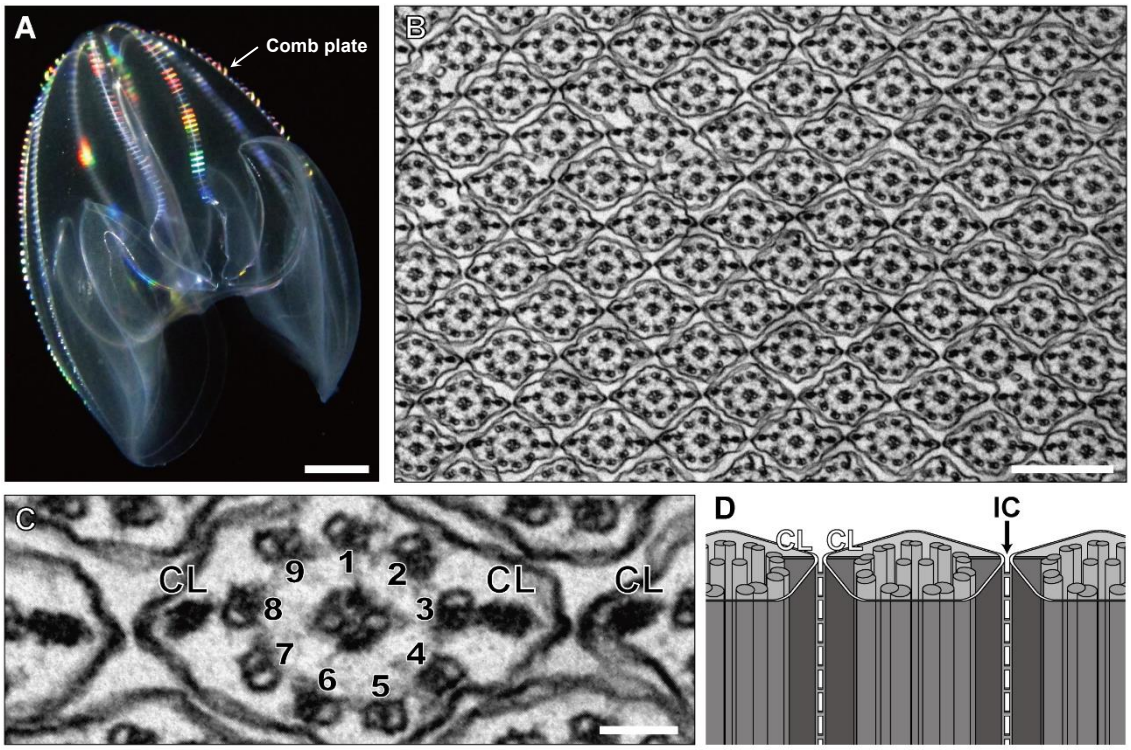

Figure 2.1 Compartmenting lamellae in the comb plate of the ctenophore *Bolinopsis mikado*

(A) A whole body of *B. mikado*. An arrow indicates a comb plate. Scale bar, 1 cm. (B) Transmission electron microscopy (TEM) of a comb plate. Scale bar, 500 nm. (C) Compartmenting lamellae (CL) are the structure connecting adjacent cilia. Doublet microtubule numbers are indicated. Scale bar, 100 nm. (D) A diagram showing the longitudinal appearance of CLs, based on the previous report (Dentler, 1981). IC, interciliary bridges.

2.2 Materials and Methods

2.2.1 Biological materials

Adults of the ctenophore, *Bolinopsis mikado* were collected by snorkeling with bottles at Oura Bay (Shimoda) or by ladling a long dipper from piers at Nanao Bay (Nanao), Hirakata Bay (Kanazawa-hakkei), Aburatsubo Bay (Misaki), and Saigo Bay (Okinoshima). Other adults of ctenophores, *Ocyropsis fusca* and *Beroe mitrata*, were collected with a long dipper from a fishing boat off the coast in Toyama Bay (Ishikawa), and *Leucothea japonica* were collected by snorkeling with bottles at Oura Bay (Shimoda).

2.2.2 Rearing of the ctenophores, *B. mikado*

Adult *B. mikado* were maintained in a 60-150 L aquarium with slowly circulating seawater. In order to maintain the seawater quality, filtered natural seawater was supplied to the aquarium at a flow rate of 150 ml/min and the excess seawater overflowed through the filter unit. The water temperature was controlled using a circulating cooler and a throw-in heater. They were fed by 10-40 ml brine shrimp (75-100 individuals/ml) a day under constant light until use. To induce sexual maturation, the brine shrimps were cultured with SCP (Pacific Trading Co., Fukuoka, Japan) and given to *B. mikado* three times a day. Mature eggs and sperm were observed in the ovary and testis along a meridional canal after a week. Four individuals were transferred to a 1-L polystyrene beaker and kept in the dark for 7-8 h, and subsequent lightning induced spawning. After the light was turned on, a small volume of seawater was collected from the bottom of the beaker every ~30 min to check the spawning of eggs and sperm with a binocular stereo microscope. Spawning usually continued for about 2 h. Fertilized eggs were collected and cultured in a petri dish and kept at 18°C until use. The fertilized eggs undergo first cleavage about 1 h after the spawning and hatch out 24 h after the lightning at 18°C.

2.2.3 Isolation of comb plates

B. mikado and *B. mitrata* were placed in ~90 mL filtered sea water. The comb plates were detached from the body surface by adding 1/5 volume of Ca^{2+}/Mg^{2+}-free sea water, containing 580.1 mM NaCl, 9.39 mM KCl, 5 mM EGTA, 5 mM EDTA, and 10 mM HEPES-NaOH at pH 8.0. In *O. fusca* and *L. japonica*, the comb plates were cut from their root with tungsten needles.

2.2.4 Extraction of comb plate proteins

The collected comb plates were washed once with filtered sea water and recovered by centrifugation at 11,110 g for 10 min at 4°C. Then the comb plates were treated with 0.1% Triton X-100 in a wash buffer (0.15 M KCl, 1 mM $MgSO_4$, 0.5 mM EGTA and 20 mM Tris-HCl at pH 8.0) on ice for 10 min and centrifuged at 11,110 g for 10 min at 4°C. The pellet (comb plate axonemes) was suspended in the wash buffer and centrifuged again. Then washing was repeated three times to remove Triton X-100. Successive extraction of the axonemes was carried out by the method of Inaba et al. (1988). The axonemes were first extracted in the wash buffer containing 0.6 M KCl and kept on ice for 30 min, followed by centrifugation at 17,360 g for 15 min. The pellet was then suspended in the wash buffer containing 1.0 M KCl and kept on ice for 30 min, followed by centrifugation at 17,360 g for 15 min.

2.2.5 Electron Microscopy

Samples were fixed with 2.5% glutaraldehyde in 0.45 M sucrose, 0.1 M sodium cacodylate (pH 7.4), washed by 0.1 M sodium cacodylate (pH 7.4), and post-fixed with 1% OsO_4 for 1 h. After dehydration in a graded ethanol series, samples were embedded in agar low viscosity resin (Agar Scientific, Stansted, UK) through propylene oxide, and thin-sectioned with an average thickness of 70 nm. Sections were stained with uranyl acetate and observed under a 1200EX electron microscope (JEOL, Tokyo, Japan) at 80 kV.

2.2.6 Protein identification by mass spectrometry

Proteins were separated by SDS-PAGE, stained with CBB, and cut out from a polyacrylamide gel into small pieces. The gel slices were sequentially treated with 50% methanol twice and 100% acetonitrile once, dried, and incubated in 10 ng/μl trypsin (Promega, WI, USA) in 25 mM NH_4HCO_3 for 16 h at 37°C. The tryptic fragments were mixed with equal volume of matrix solution containing 10 mg/ml α-cyano-4-hydroxycinnamic acid in 50% acetonitrile and 0.1% trifluoroacetic acid and subjected to MALDI-TOF/MS analysis using the Autoflex II system (Bruker Daltonics, MA, USA) in the reflector-positive ion mode. Peptides were detected and analyzed by flexControl with peptide calibration standard II. For protein identification, peptide mass fingerprinting was performed by flexAnalysis and MASCOT server 2.1 (Matrix Science, London, UK), using the transcriptome assembly sequence database of *B. mikado* and protein models (version 2.2) of the *Mnemiopsis leidyi* genome obtained through the *Mnemiopsis* genome project portal

(http://research.nhgri.nih.gov/mnemiopsis).

2.2.7 Antibodies against CTENO64

The open reading frames in the cDNA inserts were amplified by polymerase chain reaction. Primers used were 5'-GCGCGGATCCAAAAGAGTCAAAGCAAGCAA-3' (forward) and 5'-GCGCGAATTCTTACGCTTGTATTTTGCCCA-3' (reverse) for *CTENO64*. The amplified cDNA and pET 28a (+) were cleaved with *Eco*RI and *Bam*HI, purified by S-400 spin column (GE Healthcare, IL, USA), ligated with other, and electroporated into *E. coli* BL21. After checking the transformation, bacteria from a single colony were inoculated into LB medium with 50 μg/ml kanamycin and incubated at 37°C. Protein expression was induced by 1 mM isopropyl-1-thio-β-d-galactopyranoside during the logarithmic growth phase. The bacteria were harvested by centrifugation, and the recombinant CTENO64 was purified according to the method described previously (Padma et al., 2003). After dialysis against PBS, recombinant CTENO64 was emulsified with Freund's complete adjuvant and immunized to male BALB/c mice by three subcutaneous injections at intervals of 10 days. A test bleed was performed before collecting the antiserum.

2.2.8 Western blot analysis

Proteins were separated by SDS-PAGE and transferred to polyvinylidene difluoride membranes. Membranes were treated with 7.5% skim milk in PBS containing 0.1% Tween 20 (PBST). Blots were incubated with the anti-CTENO64 antibody at a 1:1000 dilution for 1 h at room temperature. After washing with PBST, blots were incubated with HRP-conjugated secondary antibody at a 1:10000 dilution for 30 min at room temperature. After washing with PBST three times, blots were developed using an enhanced chemiluminescence kit, ECL Prime (GE Healthcare, IL, USA).

2.2.9 Cross-linking experiment

The comb plate axonemes were washed with a buffer containing 0.15 M KCl, 20 mM HEPES/NaOH, 1 mM $MgSO_4$, and 0.5 mM EGTA at pH 8.0, and treated with various concentrations of BS3. The reaction was terminated by adding a 5× sample buffer for SDS-PAGE. The cross-linked products were analyzed by SDS-PAGE, followed by western blotting with the anti-CTENO64 antibody.

2.2.10 Immunofluorescence microscopy

Immunofluorescence microscopy was performed using the method previously reported (Pang and Martindale, 2008) with some modifications. Comb plates were cut from adult *B. mikado* by tungsten needles in filtered seawater and attached to a glass slide precoated with 1 mg/ml poly-l-lysine. After 5 min at room temperature, the comb plates were fixed with 4% PFA, 0.02% glutaraldehyde, 0.5 M NaCl, 0.1 M MOPS (pH 7.4) at 4°C for 1 h. The slides were washed using excess PBST. The slides were transferred to a moist chamber and incubated in a blocking buffer containing 10% goat serum in PBS for 1 h at 4°C, followed by incubation with anti-CTENO64 polyclonal antibody and anti-acetylated-α-tubulin antibody (T6793, Sigma-Aldrich, MD, USA) at 1:500 dilution in the blocking buffer overnight at 4°C. After washing with PBST at 4°C, samples were incubated with goat anti-mouse IgG (Alexa 488; Molecular Probes, Eugene, OR) and goat anti-rabbit IgG (Alexa 546; Molecular Probes) at a 1:1000 dilution for 1 h at room temperature. After washing with PBST at 4°C, samples were observed under a Fv10 confocal microscope (Olympus, Tokyo, Japan).

2.2.11 Immunogold Labeling

For post-embedding immunogold labeling, isolated adult comb plates were fixed with 4% PFA, 0.02% glutaraldehyde, 0.4 M sucrose, 0.1 M cacodylate buffer (pH 7.4), washed several times with 0.1 M cacodylate buffer (pH 7.4) and post-fixed with 1% OsO_4, 1.5% sodium ferrocyanide, 0.1 M cacodylate buffer (pH 7.4) for 30 min on ice. After being washed with 0.1 M sodium cacodylate (pH 7.4), samples were dehydrated through a graded ethanol series and embedded in LR-white at 55°C for 48 h. The block was thin-sectioned with an average thickness of 70 nm and deposited on a nickel grid (300 mesh) supported by formvar films. The sections were pre-treated for etching with a saturated aqueous solution of sodium metaperiodate for 1 min, followed by five washes in distilled water. Then they were sequentially treated with 1% BSA in PBS for 1 h, primary anti-CNENO64 antibody (1:1000 dilution) at 4°C overnight, four times with PBS and anti-mouse secondary antibody conjugated with 5 nm colloidal gold particle (BBI, UK, 1:50 dilution) for 1 h. After washing with PBS, the sections were stained with 5% aqueous uranyl acetate for 5 min and observed under EM.

Pre-embedding immunogold labeling was performed as previously reported (Padma et al., 2003), with some modifications. The comb plate was demembranated using 0.2% Triton X-100 in 150 mM KCl, 2 mM $MgSO_4$, 0.5 mM EGTA, 10 mM HEPES (pH 8.0). After washing twice with Triton-free buffer and PBS, the comb plates were fixed with 0.1% glutaraldehyde in PBS for 1 h at 4°C. After

washing with PBS three times, samples were treated with 1 mg/ml $NaBH_4$ in PBS for 10 min at room temperature and washed twice with PBS. Samples were incubated in a blocking buffer containing 1% BSA, 1% goat serum in PBS for 2 h at 4°C with occasional agitation. After being washed with PBS, the samples were incubated with control IgG, anti-CTENO64 antibody (1:50 dilution) in blocking buffer for 12 h at 4°C, then washed with blocking buffer four times and incubated at 4°C for 12 h with 5-nm-gold conjugated anti-mouse IgG (1:20 dilution). They were then washed with blocking buffer and fixed with 2.5% glutaraldehyde in 0.45 M sucrose, 0.1 M cacodylate buffer (pH 7.4), at room temperature for 1 h. Samples were post-fixed with 1% OsO_4 in 0.1 M cacodylate buffer for 1 h, dehydrated in a graded ethanol series, embedded in agar low viscosity resin through propylene oxide, and thin-sectioned with an average thickness of 70 nm. The sections were stained with uranyl acetate and observed under EM.

2.2.12 Microinjection of morpholino antisense oligonucleotide (MO)

Two morpholino antisense oligonucleotides MO1 (5'-ACAGTGCTCACAAATAACGAACA GA-3') and MO2 (5'-ATAGTCAGAGCTTTTCGCACTTCGT-3') were designed to cover the 5'-UTR region of the *B. mikado CTENO64* mRNA (Gene Tools, Philomath, OR, USA). MOs were suspended in distilled water and stored in a freezer. An aliquot of MOs was thawed and heated to 65°C for 10 min to ensure that they were completely dissolved. Microinjections were performed with pressure using the method reported previously (Martindale and Henry, 1997) with some modifications. MOs were dissolved in 0.4 M KCl and 40% glycerol to 1 mM and injected to fertilized eggs with vitelline membrane before cleavage. The injection volume was controlled by measuring the diameter of each droplet injected. The final concentration of MO in an egg was ~3.5 μM. Eggs were kept in filtered sea water (FSW) at 18°C for further development.

2.2.13 Analysis of larval swimming behavior and ciliary beating

The larvae at 30 hpf were placed in a 35-mm plastic dish at 18°C. The motility of the comb plate was recorded using a binocular microscope (MZ12.5, Leica) equipped with a high-speed camera (500 frames per second; HAS-220, DITECT). The waveforms were traced and analyzed using Bohboh software (Bohboh Soft, Tokyo, Japan), as described previously (Mizuno et al., 2017).

2.2.14 Comparison of ciliary orientation

For analysis of ciliary orientation in larvae, the angles between the axis of two singlet microtubules (direction of doublet 8 to 3) and the aboral-oral axis of larvae were measured. Data were compared using circular histograms as described previously (Mizuno et al., 2017).

2.3 Results

2.3.1 Selective extraction of comb plate reveals candidates for CL components

I used the ctenophore *Bolinopsis mikado* (Fig. 2.1A), a species in the order Lobata alongside *Mnemiopsis leidyi*, which is one of the ctenophore species with full genome sequence information available (Ryan et al., 2013). A comb plate of adult *B. mikado* is constructed from ~50,000 cilia, estimated from the images of thin-sectioned transmission electron microscopy (TEM) (Fig. 2.1B). CLs extend from two doublet microtubules (doublet 3 and 8) toward the plasma membrane and connect to the doublet microtubules of adjacent ciliary axoneme through interciliary bridges (Fig. 2.1C, D). The doublet 3−8 plane represents the same plane as the central apparatus and is perpendicular to the oral−aboral direction of the ciliary beating plane (Afzelius, 1961).

I established a system for rearing *B. mikado* and a procedure for biochemical dissection of comb plates. Comb plates were detached from the body surface by the addition of Ca^{2+}/Mg^{2+}-free artificial sea water (Linck et al., 1991). The isolated comb plates were treated with Triton X-100 to remove the plasma membrane and was followed by chemical dissection (Gibbons, 1972; Inaba et al., 1988; Stephens, 1970) of the ciliary axonemes with salt extractions. TEM revealed that CLs were mostly extracted from the axonemes by 1.0 M KCl after 0.6 M KCl treatment that removed the outer arm dyneins (Fig. 2.2).

SDS-PAGE revealed six major proteins rich in this fraction (Fig. 2.3). I identified these proteins by MALDI-TOF/MS using a protein database that was constructed from the transcriptome of embryos, hatched larvae, and comb plate cells. These included the 53- and 52-kDa α- and β-tubulins and the 49- and 47-kDa tektins, but also included a 76-kDa protein showing sequence homology to a hemocyanin and a 64-kDa protein that was not significantly homologous to any known proteins (Table 2.1).

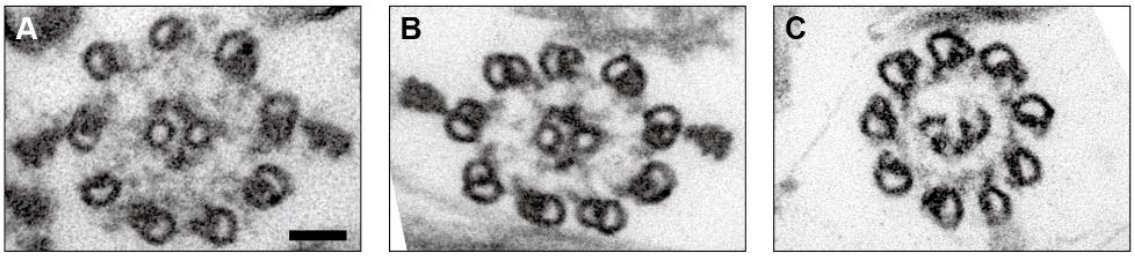

Figure 2.2. TEM images of the comb plate axoneme after selective extractions

TEM images of the comb plate after sequential treatment by Triton X-100 (A), 0.6 M KCl (B), and 1.0 M KCl (C) solutions. The CL were extracted from 0.6 M KCl solution-treated axonemes by 1.0 M KCl solution. Bar, 100 nm.

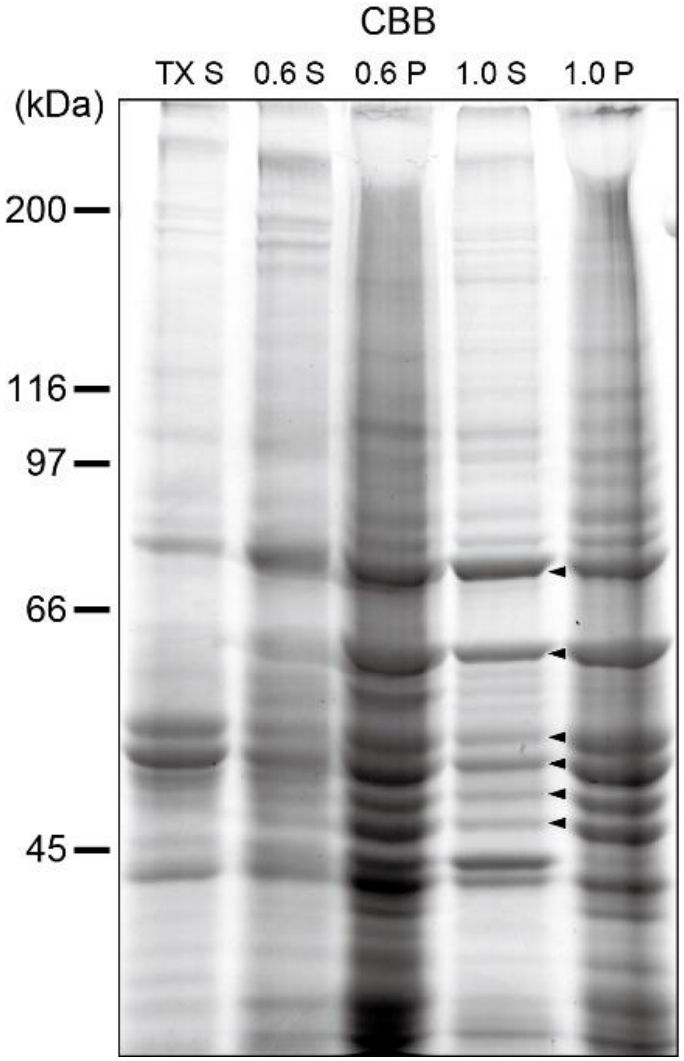

Figure 2.3. Protein patterns of the extracts after the sequential treatments of the comb plates

Protein patterns of the extracts after the sequential treatments by Triton X-100 (TX), 0.6 M KCl (0.6), and 1.0 M KCl (1.0) solution. (S, supernatant; P, pellet). CBB, protein staining with Coomassie Brilliant Blue. Black arrowheads indicate the proteins subjected to MALDI-TOF/MS analysis.

Table 2.1. Identification of the candidates for CL components by MALDI-TOF/MS

Protein band (kDa)	ID	Mass	MASCOT search			BLASTP search		
			Score	Expect	Matches	Description	Expect	Identity (%)
76	c53371_g1_i1	82485	181	2.9E-14	24	PREDICTED: phenoloxidase 3-like [Drosophila suzukii]	6.0E-90	32
64	c57141_g1_i1	58574	254	1.4E-21	27	Not significant		
53	c50927_g3_i2	33632	69	4.5E-03	8	PREDICTED: tubulin alpha-1A chain [Ciona intestinalis]	0.0	97
52	c46007_g5_i1	15636	67	7.3E-03	7	PREDICTED: tubulin beta-4A chain-like [Salmo salar]	8.0E-99	99
49	c47946_g1_i2	52214	91	2.6E-05	13	Tektin-1 [Exaiptasia pallida]	6.0E-108	46
47	c47946_g1_i2	52214	116	9.0E-08	14	Tektin-1 [Exaiptasia pallida]	6.0E-108	46

2.3.2 CTENO64 is a ctenophore-specific coiled-coil CL protein

The 64-kDa protein was a coiled-coil protein with two coiled-coil regions from amino acid residue 235−291 and 370−453 but was not homologous to any known proteins (Accession number: LC462191 in the DDBJ/GenBank/EMBL database). It contained an SMC_N superfamily domain from amino acid 244−451, which is potentially involved in the formation of a dimer structure (Fig. 2.4) (Hirano and Hirano, 2002). Local BLAST searches for the published transcriptome data of four other ctenophore species, *Bolinopsis infundibulum*, *Beroe abyssicola*, and *Pleurobrachia pileus* (https://neurobase.rc.ufl.edu/) showed that homologs of CTENO64 were found in all of them (Table 2.2), with the highest hit found in *M. leidyi* (registered as ML049618a in the *Mnemiopsis* Genome Project Portal). Considering that this 64-kDa protein is uniquely present in ctenophore species, I named it as CTENO64 (for ctenophore 64-kDa protein). The anti-CTENO64 antibody specifically recognized the 64-kDa protein in a 1.0 M KCl fraction, confirming the result obtained from selective extraction (Fig. 2.5).

The antibody cross-reacted with proteins in other ctenophore species, *Ocyropsis fusca* (Ocyropsidae, Lobata), *Leucothea japonica* (Leucotheidae, Lobata), and *Beroe mitrata* (Beroida) (Fig. 2.6). The molecular mass of the CTENO64 ortholog in *L. japonica* were almost the same as that of *B. mikado*; those of *O. fusca* and *B. mitrata* showed slightly lower (Fig. 2.6D).

A cross-linking experiment was done in order to know the molecular interaction of CTENO64 in the comb plate. A crosslinker, bis(sulfosuccinimidyl)suberate (BS3), generated a 129-kDa cross-linked product, suggesting that CTENO64 may form a dimer in CL in the axonemes of a comb plate (Fig. 2.7). Increasing the BS3 concentration further generated a very high molecular mass product, suggesting the interaction of CTENO64 with other proteins within the comb plate.

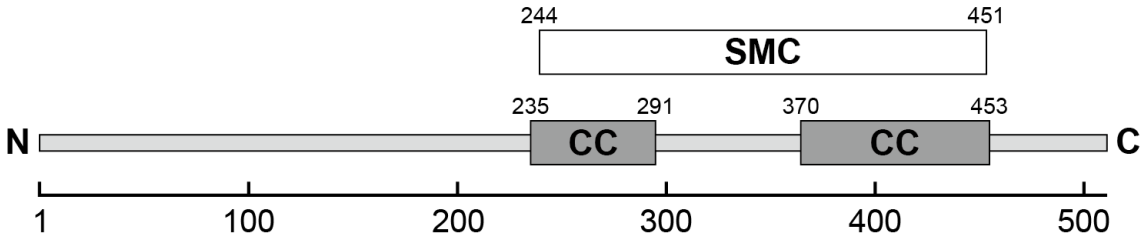

Figure 2.4. CTENO64 is a ctenophore-specific coiled-coil protein

The domain structure predicted for CTENO64. CTENO64 has two coiled-coil domains (CC) from amino acid (AA) 235–291 and AA 370–453 (predicted by the program COILS). These regions match with an SMC_N superfamily domain (SMC) (AA 244–451) in the NCBI conserved domain search, which is potentially involved in the formation of a dimer structure.

Table 2.2. Homology search for the orthologous genes of CTENO64 in other ctenophores

Species	ID	Length (a.a.)	Score	Expect	Identity (%)
Mnemiopsis leidyi	ML049618a	498	886	0.0	90
Bolinopsis infundibulum	Bi_70921_c0_seq22	636	846	0.0	83
Beroe abyssicola	Ba_18173_c0_seq9	544	737	0.0	71
Pleurobrachia pileus	Pp_46139_c2_seq9	961	657	0.0	64

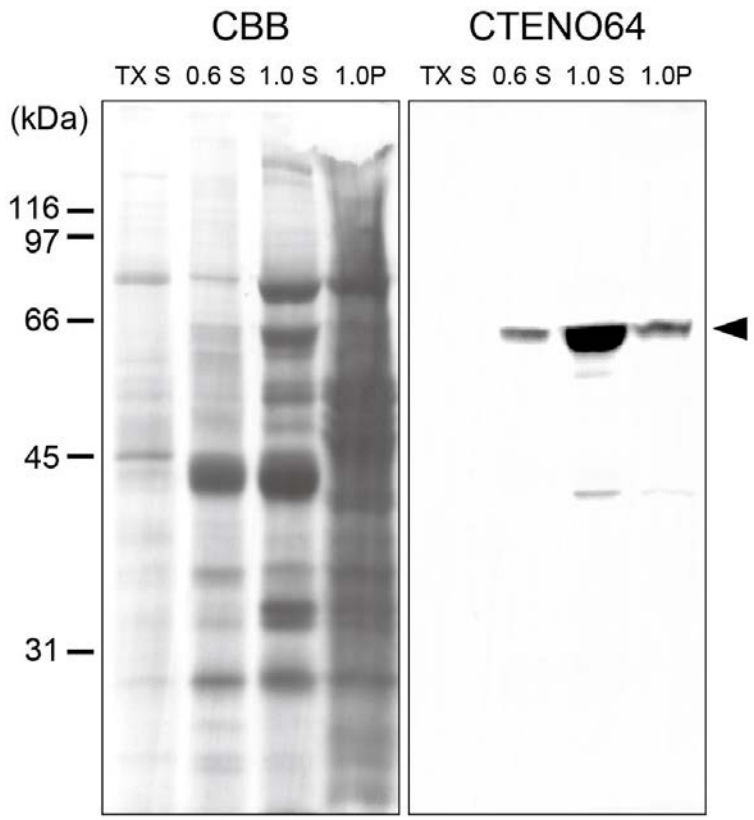

Figure 2.5. Western blot analysis with a polyclonal anti-CTENO64 antibody

CTENO64 was detected in a 1.0 M KCl extract (arrowhead). TX, Triton X-100; 0.6, M KCl solution; 1.0, 1.0 M KCl solution; S, supernatant; P, pellet.

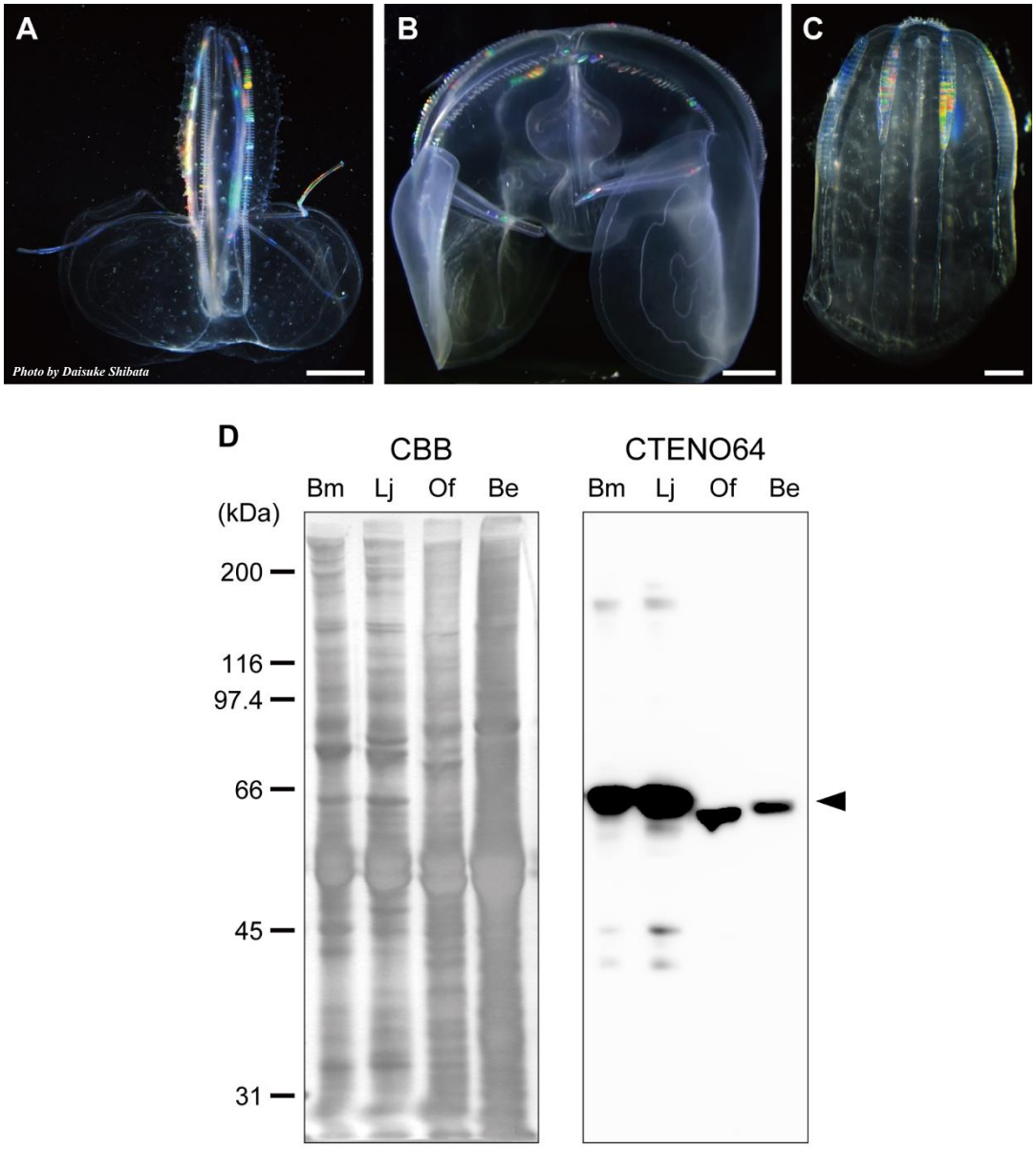

Figure 2.6. Western blot analysis of CTENO64 in other ctenophores

(A) *Leucothea japonica*. Scale bar, 2 cm. (B) *Ocyropsis fusca*. Scale bar, 1 cm. (C) *Beroe mitrata*. Scale bar, 0.5 cm. (D) Western blot analysis of CTENO64 in other ctenophore species. CBB, protein staining with Coomassie Brilliant Blue of the comb plate whole proteins from *B. mikado* (Bm), *L. japonica* (Lj), *O. fusca* (Of) and *B. mitrata* (Be). CTENO64, western blotting with the anti-CTENO64 antibody. CTENO64 was detected in all four species.

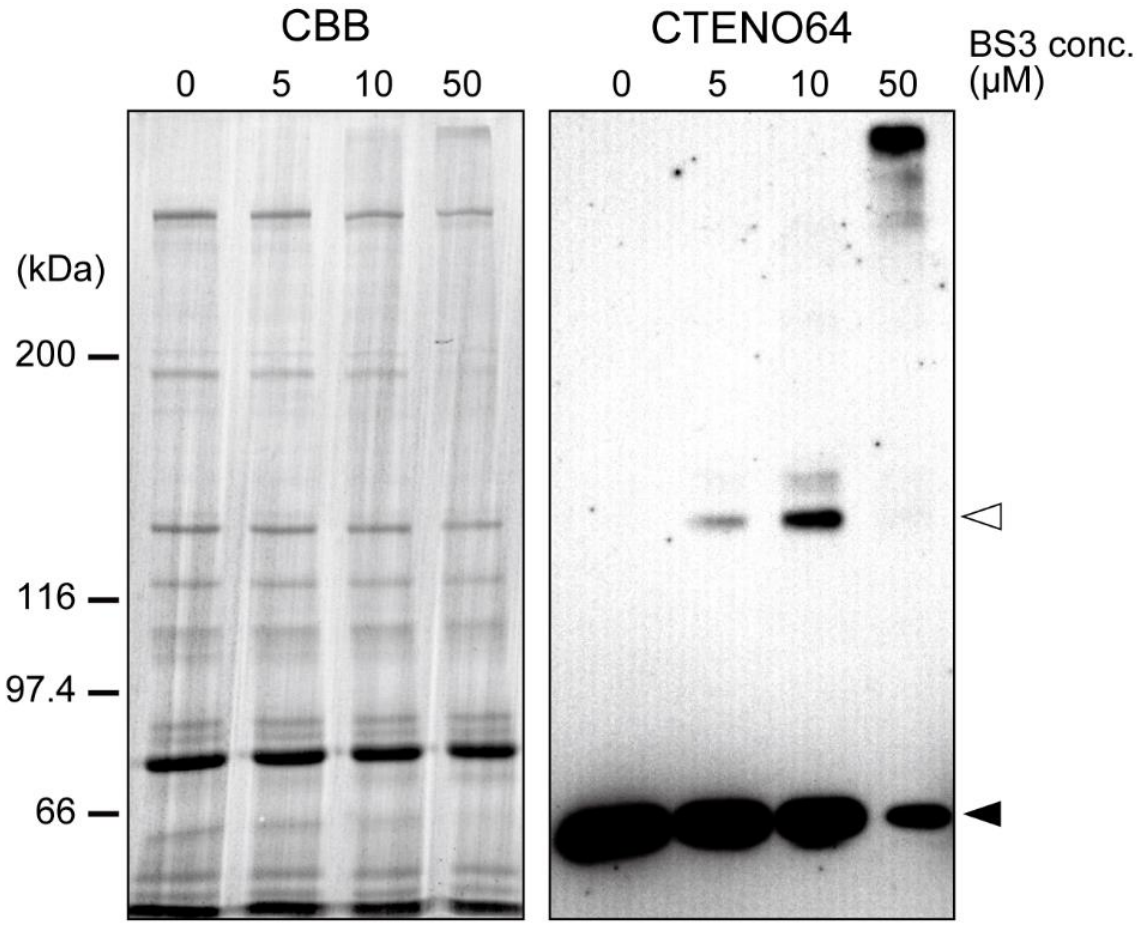

Figure 2.7. Chemical crosslinking analysis of CTENO64

Analysis of protein-protein interaction with a crosslinker, BS3. Triton-extracted comb plates were treated with a solution containing BS3 with different concentrations for 1 h at 4°C. Closed arrowhead, CTENO64; open arrowhead, a 129 kDa cross-linked product of CTENO64. CBB, protein staining with Coomassie Brilliant Blue. CTENO64, western blotting with the anti-CTENO64 antibody.

2.3.3 CTENO64 is localized at CL in the proximal part of comb plate

Immunofluorescence microscopy showed that CTENO64 was specifically localized in the proximal around one sixth to one tenth region of the adult comb plate and was not found in other cilia, including those in the pharynx (Fig. 2.8). The length of the fixed adult comb plate was about 800 μm, of which CTENO64 was strongly localized to the region of 80-120 μm from the base of a comb plate. Immunogold localization revealed the presence of gold particles on the CL (Fig. 2.9).

2.3.4 CTENO64 is required for CL formation but not for comb plate ciliogenesis

To determine the function of CTENO64 in the formation and motility of comb plates and in the molecular architecture of CLs, I knocked down its expression using morpholino oligonucleotides (MO). MOs were injected into fertilized eggs and the embryos were cultured for up to 30 h post-fertilization (hpf). CTENO64 expression in a comb plate was greatly reduced, although the formation of comb plates was apparently normal (Figs. 2.10, 2.11A, 2.13A). Neither the number of comb plates per comb row (six in four comb rows at the sagittal plane and five in those at the tentacular plane), nor their length (62.7 ± 3.6 μm for control, n = 19; 63.7 ± 2.2 μm for MO1, n = 32; Fig. 2.11B) at 30 hpf was significantly different between the control and morphant larvae. However, TEM of CTENO64 morphant larvae showed that 15.8% of the comb plate cilia lacked CLs (Figs. 2.12, 2.13B). Some cilia had half-rotated or caracole orientations in the proximal region of a comb plate (Fig. 2.12). These results suggest that CTENO64 is not directly involved in the formation of comb plates but is essential for the formation of CLs and the orientation of cilia in the comb plate.

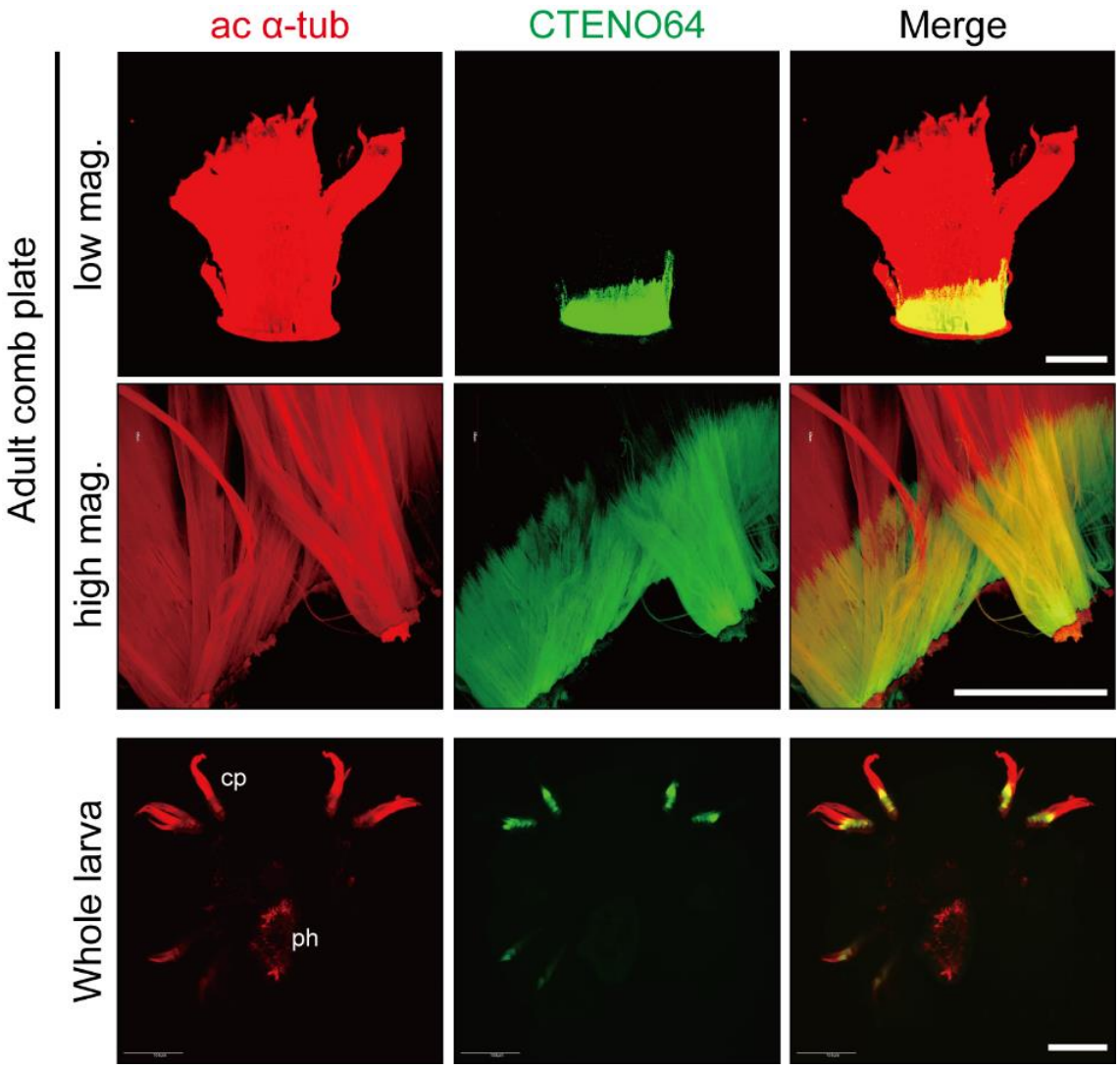

Figure 2.8. Immunofluorescence localization of CTENO64

The adult comb plate (upper, low magnification; lower, high magnification of the proximal part) and the whole larva (72 hpf) were fixed and stained with an anti-acetylated α-tubulin antibody (ac α-tub: red) and anti-CTENO64 antibody (CTENO64: green). CTENO64 is localized in the proximal region of comb plates. cp, comb plate; ph pharynx. Bar, 100 μm.

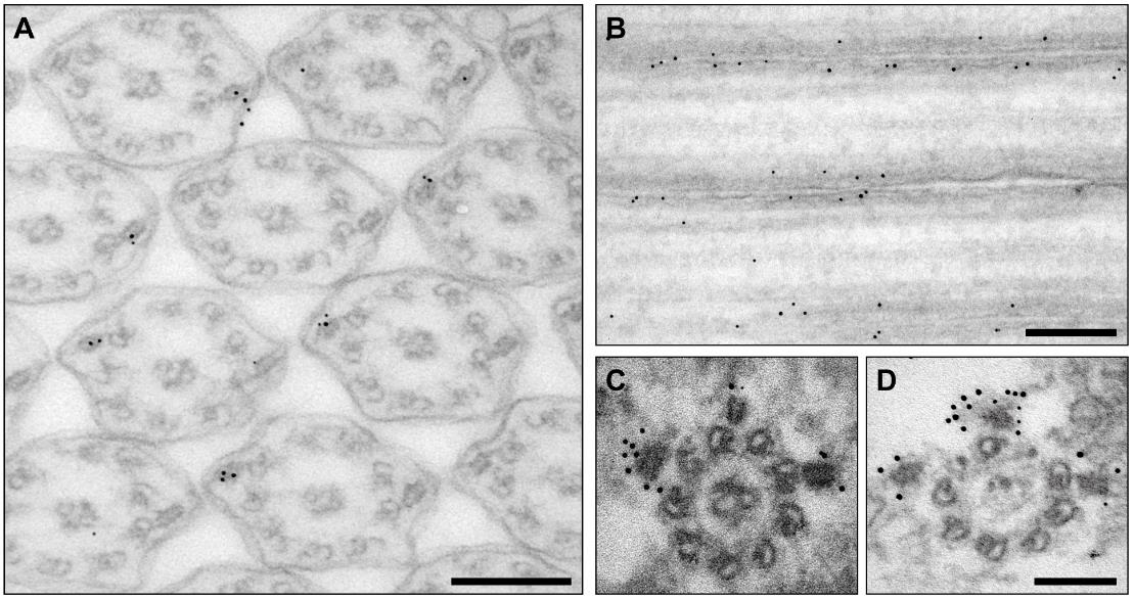

Figure 2.9. Immunogold localization of CTENO64

(A, B) Post-embedding immunogold labeling of the comb plate with the anti-CTENO64 antibody. (A) The gold particles were clearly found on the CL extending from the axonemes. Bar, 200 nm. (B) The gold particles were clearly found on the CLs in the space between each cilium. Bar, 200 nm. (C, D) Pre-embedding immunogold labeling of the comb plate with the anti-CTENO64 antibody. Only the magnified images around one axoneme are shown. Bar, 100 nm. (A, C, D) Cross sections, (B) longitudinal section.

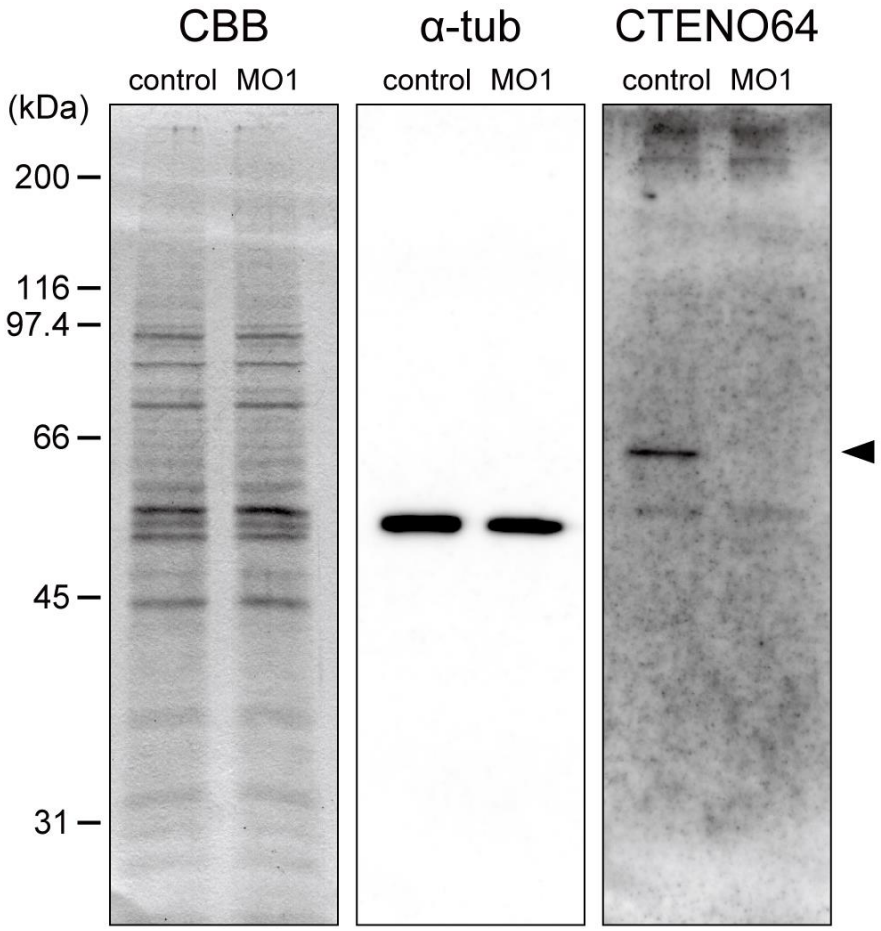

Figure 2.10. Western blot analysis of the control and CTENO64 morphant larvae

Immunoblots of the control and CTENO64 morphant larvae (MO1) (30 hpf, each 20 larvae) by anti-α-tubulin (α-tub) and anti-CTENO64 antibodies. Arrowhead, CTENO64.

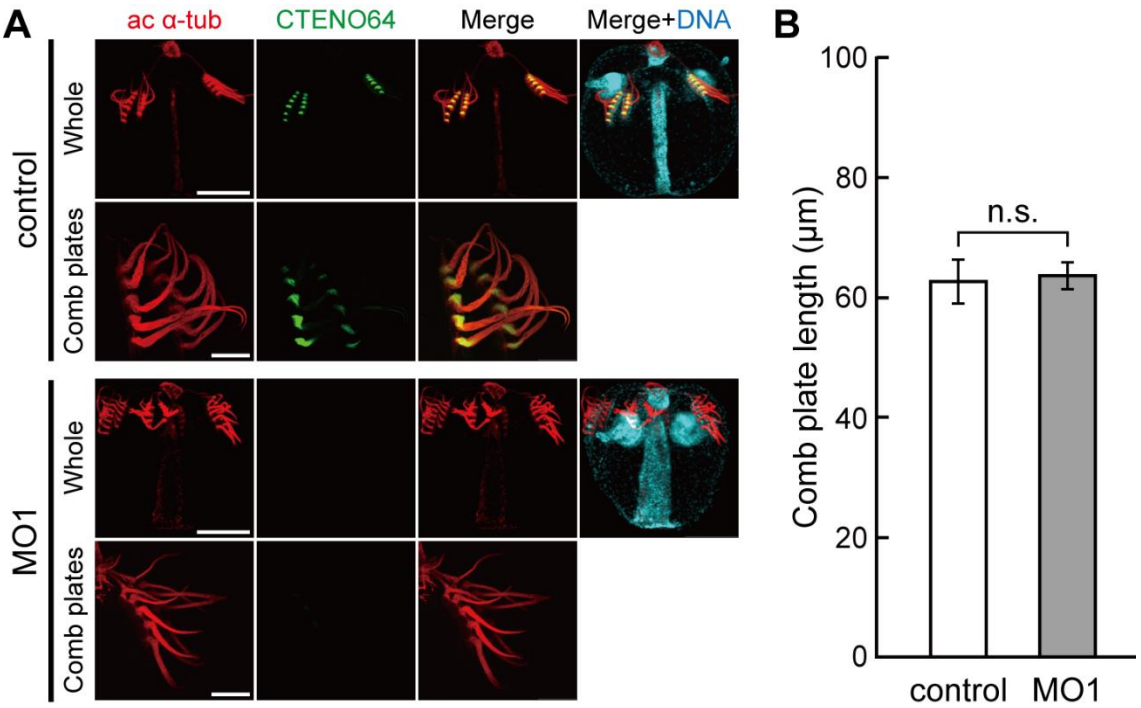

Figure 2.11. Immunofluorescence images and the length of the comb plates

(A) Immunofluorescence comparison between the control and CTENO64 morphant larvae (MO1). The larvae were stained with antibodies against acetylated α-tubulin (ac α-tub, red), an antibody against CTENO64 (green) and with DAPI for DNA. "Whole," whole larva; "Comb plates," enlarged image of the comb plate. Bar, 100 μm (Whole); 30 μm (Comb plates). (B) Average lengths of the comb plates show no difference between the control (62.7 ± 3.6 μm, n = 19) and CTENO64 morphant larvae (MO1, 63.7 ± 2.2 μm, n = 32). Error bars represent S.E. Differences between samples were statistically evaluated by t test. n.s., not significant.

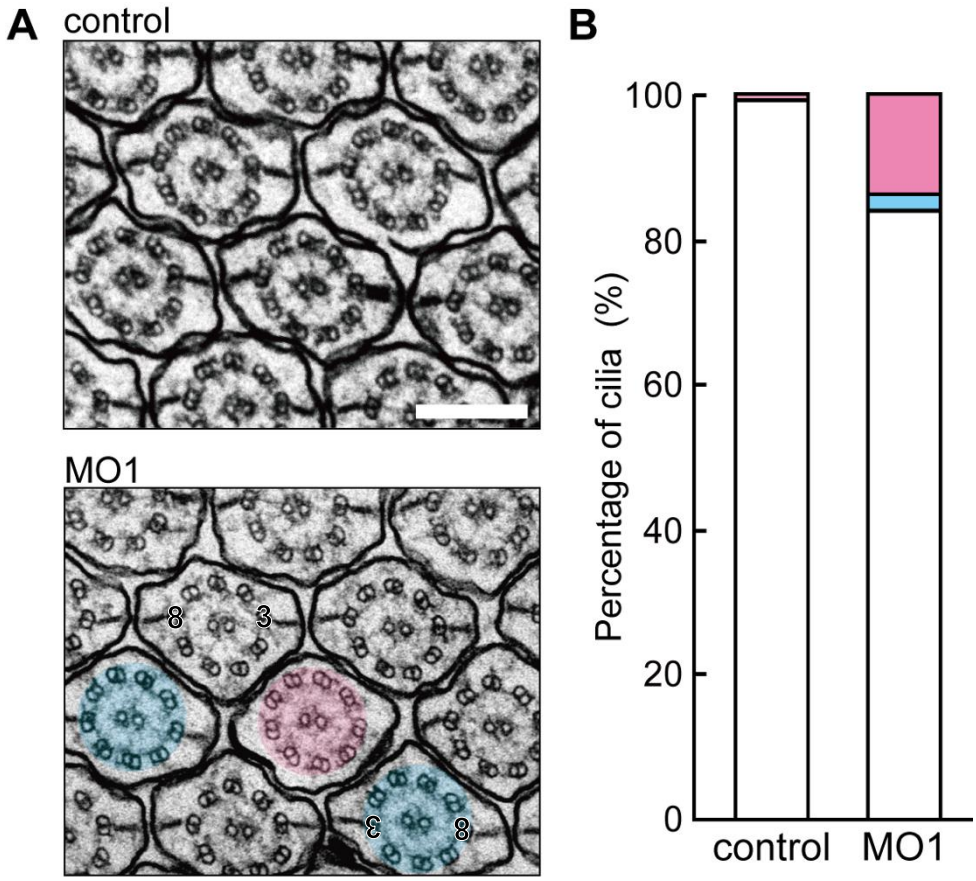

Figure 2.12. Comparison of TEM image comb plates between control and CTENO64 morphant (A) Transmission electron microscopy (TEM) images of the proximal part of a comb plate show the presence of cilia lacking CL (pink) and those with inverted orientation (blue) in the CTENO64 morphant larvae (MO1). The numbers of doublet microtubules are indicated for clarify. Bar, 200 nm. (B) Frequency of aberrant CL in the comb plate of the control (n = 444) and CTENO64 morphant larvae (MO1, n = 573). White, CL-bearing cilia with normal orientation; pink, CL-deficient cilia; blue, cilia with inverted orientation.

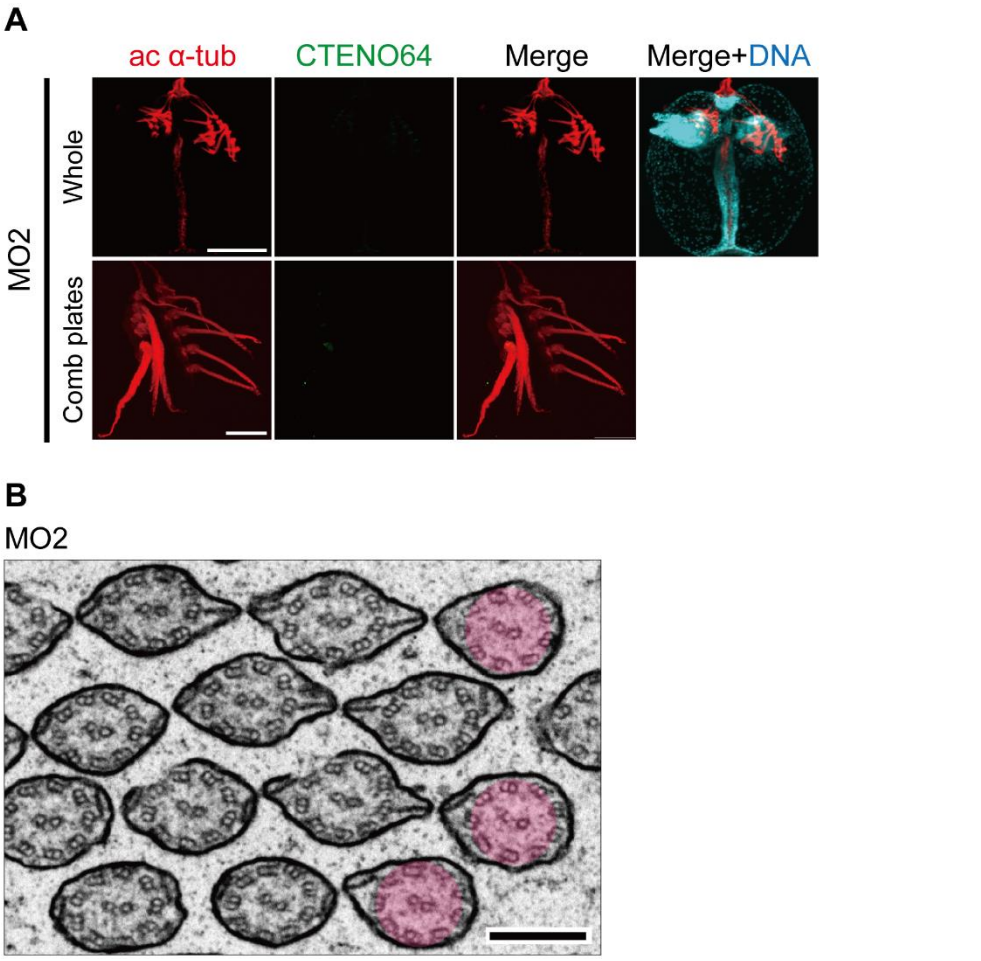

Figure 2.13. Phenotype of CTENO64 MO2 morphant larva

(A) Immunofluorescent microscopy showing suppression of CTENO64 in the comb plates of MO2 morphant larva. The larvae were stained with antibodies against acetylated α-tubulin (ac α-tub, red), CTENO64 (green) and with DAPI for DNA. "Whole," whole larva; "Comb plates," enlarged image of the comb plate. Bar, 100 μm (Whole); 30 μm (Comb plates). (B) A transmission electron microscopy (TEM) image of the proximal part of a comb plate shows the presence of cilia lacking either or both CLs (pink) in the CTENO64 morphant larva. Bar, 200 nm.

2.3.5 Loss of CL induces aberrant motility of comb plates

To determine the role of CTENO64 during ciliary movement, I recorded the movements of comb plates and compared motility parameters between the control and CTENO64 morphant larvae. I first estimated the efficiency of comb plate beating by measuring both the angle of effective stroke and beat frequency (Fig. 2.14). The angle of effective stroke was 111.3 ± 4.1° in the morphant larvae, and was not significantly different from that of the control larvae (116.7 ± 5.3°; Fig. 2.14B). Similarly, the beating frequency of a comb plate was 16.8 ± 0.9 Hz in the control and 18.0 ± 0.8 Hz in the CTENO64 morphant larvae (Fig. 2.14C).

Although the antiplectic metachronal coordination of comb plates beating along a comb plate row was not lost in the morphant larvae (Fig. 2.15), locomotion was observed to be erratic. The range of locomotion in the control larvae from the origin was up to ~30 μm in 200 msec, but that of the morphant larvae was less than 10 μm, mostly within 5 μm, and they crept around the origin (Fig. 2.16)

To elucidate the cause of the observed differences in locomotion between the control and morphant larvae, I analyzed the ciliary waveforms during a ciliary beating cycle (Fig. 2.17A). One cycle of ciliary beating consists of an effective and a recovery stroke, between which the former exerts the propulsive force for locomotion. I traced the ciliary waveforms and found that the waveform of the effective stroke was different between the control and the morphant larvae. In particular, the comb plate in the middle and at the distal end showed a strong curvature, and reversed direction of bending in the morphant larvae (Fig. 2.17B).

Some comb plates in the morphant larvae had aberrant beating planes that were often outside the microscopic focal plane (Fig. 2.18A). Approximately 14% of the comb plates in the CTENO64 morphant larvae were beating in a different plane. However, these out-of-focus ciliary beatings were not observed in the control comb plates (Fig. 2.18B).

The beating plane of cilia is determined by the orientation of the central apparatus of the ciliary axonemes (Porter and Sale, 2000). Therefore, I examined the axonemal orientations at the middle to distal end of a comb plate in both the control and the morphant larvae. TEM images showed that the planes of the central pair of microtubules in the control larvae were perpendicular to the beating plane of the comb plate (Fig. 2.19A). The cilia with normal CLs and those deficient in CLs in the morphant larvae also had a similar orientation. However, the orientation of the cilia that had caracole orientations became perpendicular to those of other cilia in a comb plate (Fig. 2.19A). Circular histograms indicated that 80.2% of the cilia were on the perpendicular plane in the control larvae, whereas the

misalignments reached 46.7% in the morphant larvae, among which 11.2% of cilia were observed to have reversed orientation (Fig. 2.19B).

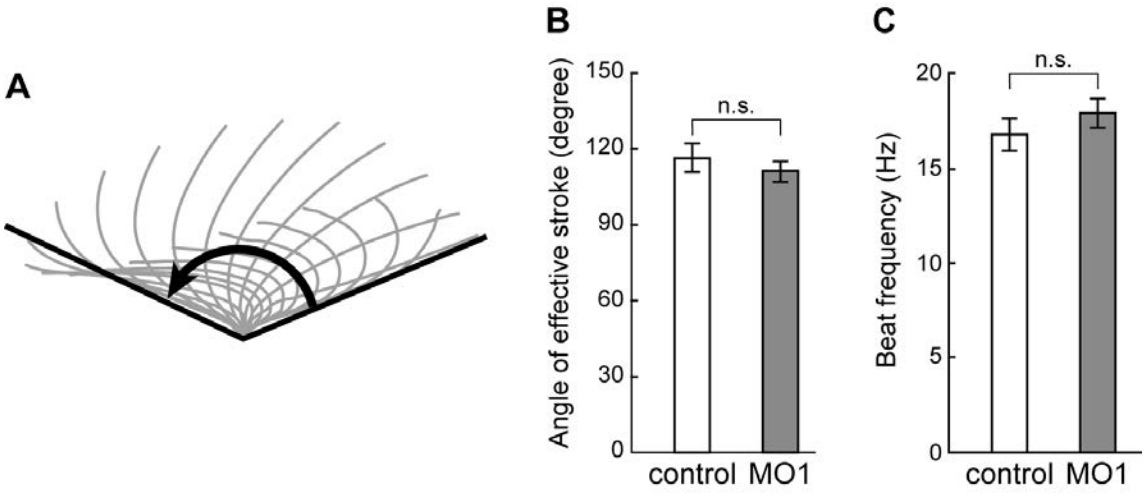

Figure 2.14. Analysis of ciliary beating and waveform of the comb plates

(A) Definition of the angle of effective stroke. (B) Comparison of the angle of effective stroke in the comb plate beating between the control and CTENO64 morphant larvae (MO1). n = 19 (control), 32 (MO1). Error bars represent S.E. (C) Comparison of the comb plate beat frequency between the control and CTENO64 morphant larvae (MO1). n = 19 (control) and 32 (MO1). Error bars represent S.E. Differences between samples were statistically evaluated by t test. n.s., not significant.

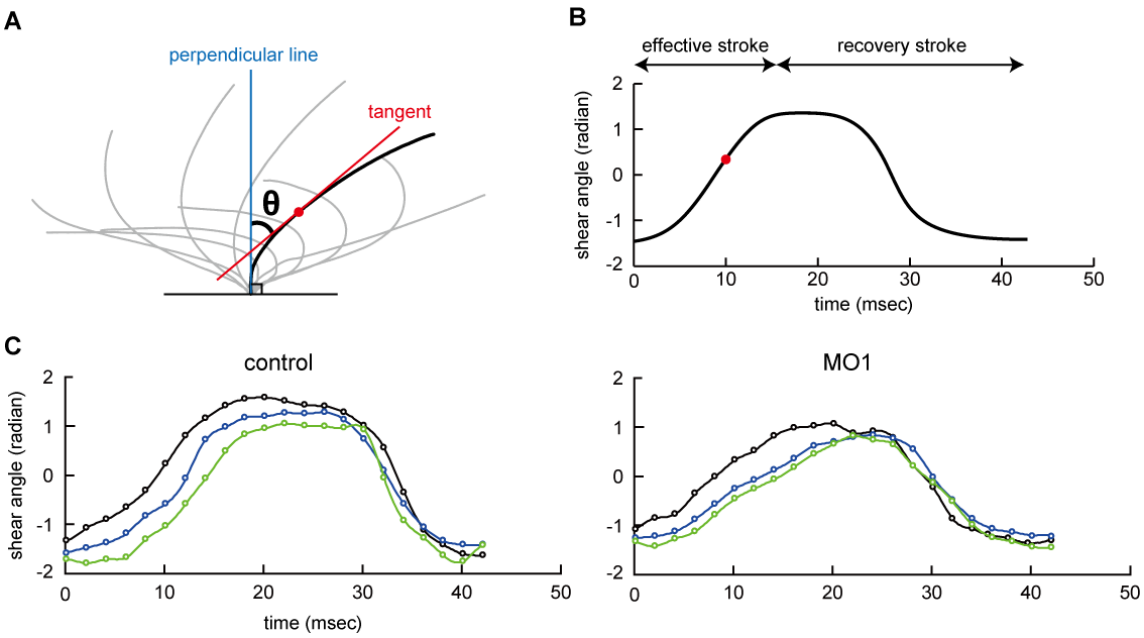

Figure 2.15. Metachronal rhythm of comb plates in a comb row

(A) Definition of shear angle (θ) at a certain point (a red dot) of a cilium during beating. (B) The expected change in shear angle during one beating cycle at a certain point (a red dot). (C) Examples of the changes in shear angles at the middle point during one beating cycle of three adjacent comb plates along a comb row in the control and morphant larvae (MO1), showing metachronal coordination in both cases. The black, blue and green curves represent the changes in shear angle of three sequential comb plates from aboral to oral direction.

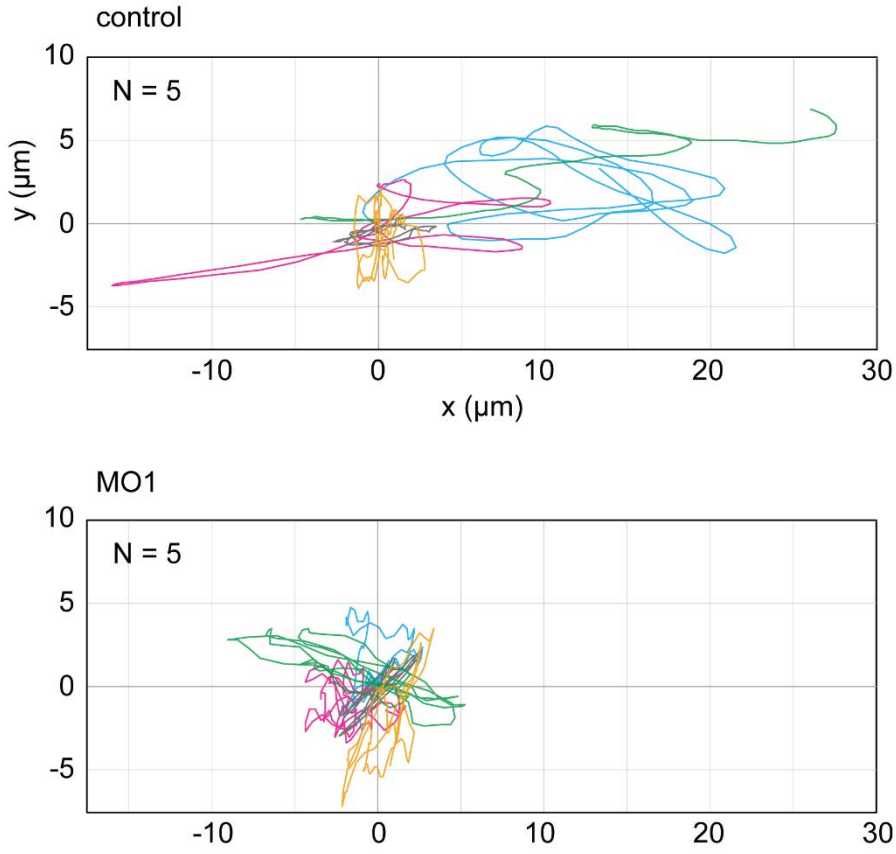

Figure 2.16. Analysis of larval locomotion

Locomotive trajectories of five control (upper) and morphant larvae (lower; MO1) for 200 msec. The origin (x = 0, y = 0) represents the initial position on the recordings. Trajectory of each individual is shown in different color.

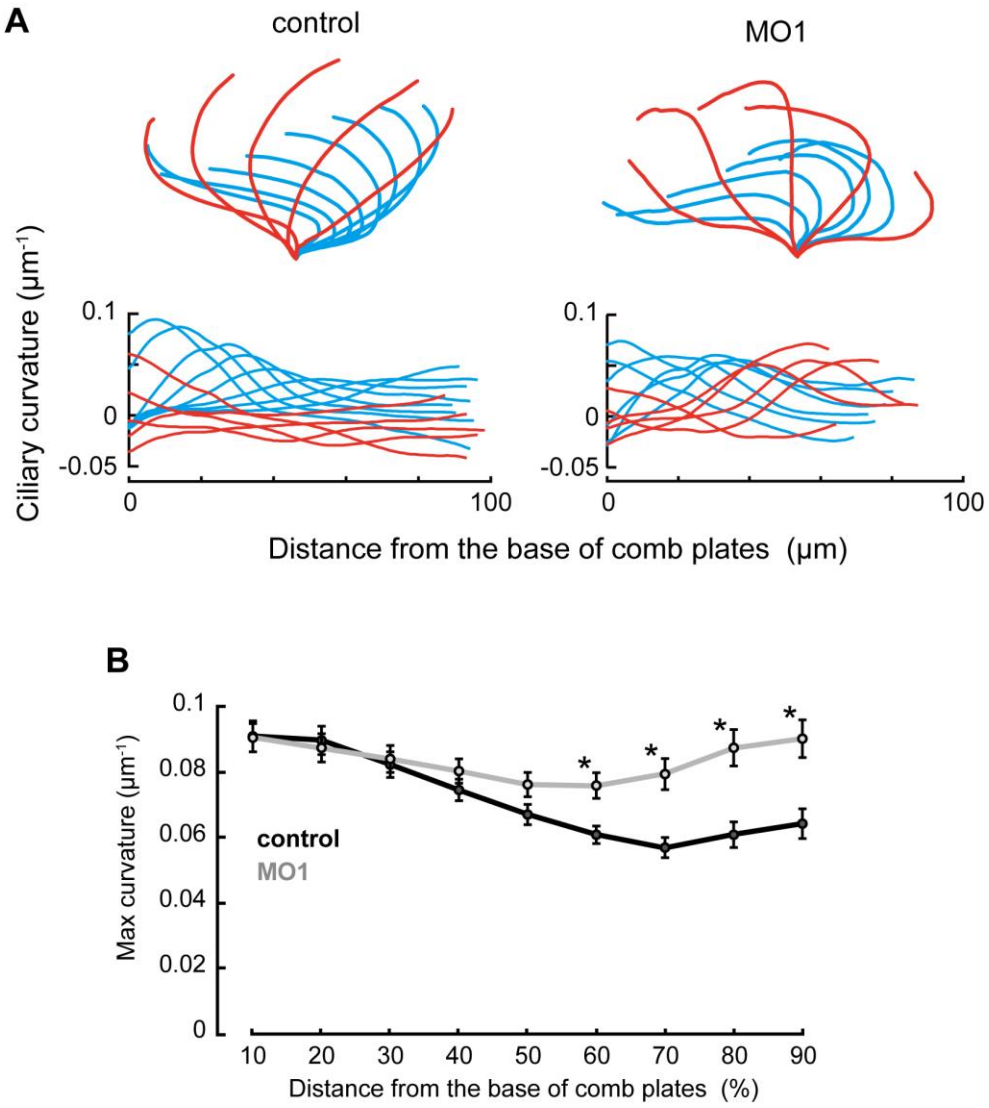

Figure 2.17. Analysis of the comb plate waveform

(A) Comparison of comb plate ciliary waveforms between the control and CTENO64 morphant larvae (MO1). The figure represents a typical beating pattern of comb plate in each larva. Upper, typical waveforms during ciliary beating; lower, the ciliary curvature along the length of a comb plate. Red and blue represent effective and recovery strokes, respectively. (B) The maximum ciliary curvature along the comb plates in the control and CTENO64 morphant larvae (MO1). The values were measured and plotted at every 10% from the bases of the full length of the comb plates. n = 19 (control) and 32 (MO1). Error bars represent S.E. Differences between samples were statistically evaluated by t test. *$p < 0.001$ vs control.

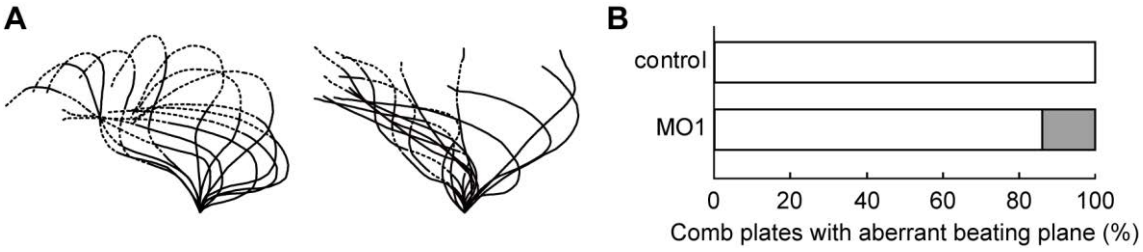

Figure 2.18. Three-dimensionality of the comb plate beating in CTENO64 morphant larvae

(A) Examples of the comb plate waveforms in CTENO64 morphant larvae showing non-planar beating. The traces of comb plate waveforms out of the microscopic focal plane are indicated by dotted lines. (B) Frequency of aberrant beating planes in the control and CTENO64 morphant larvae (MO1) of comb plates. White and gray bars indicate the percentage of comp plates fully on the focal plane and of those outside the focal plane, respectively. n = 200 (control) and 547 (MO1).

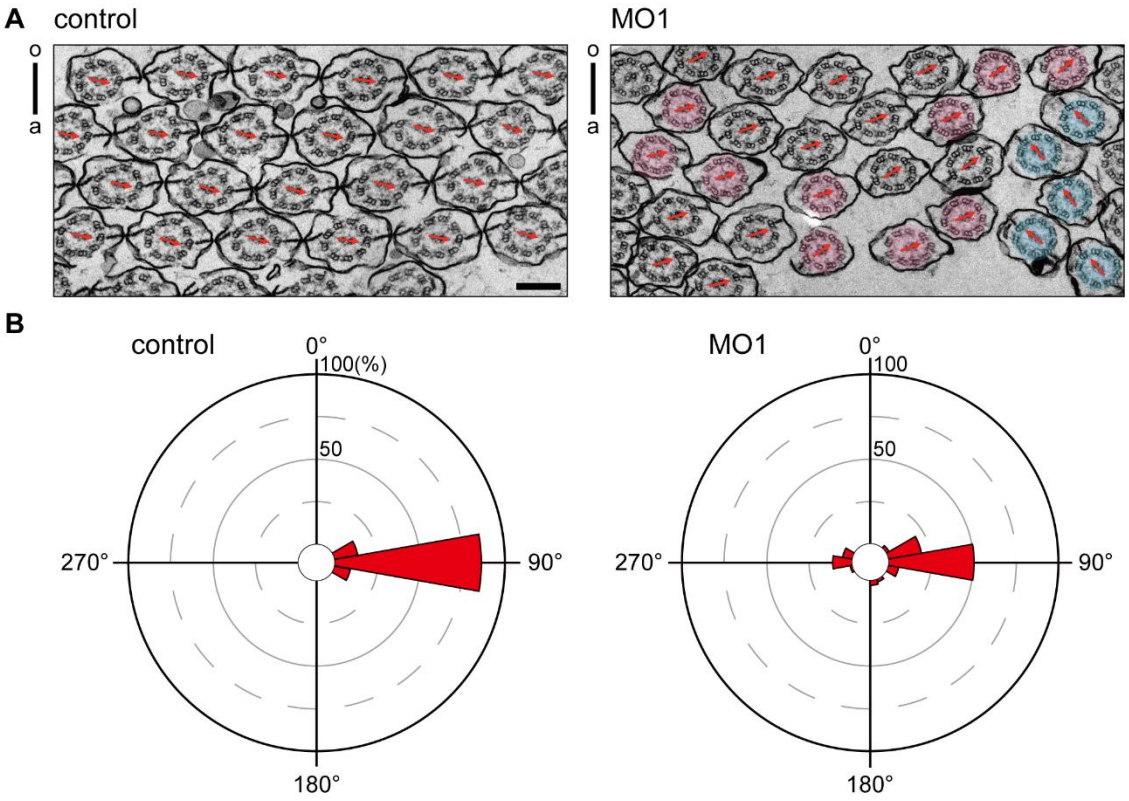

Figure 2.19. Analysis of the axonemal orientations in the comb plates

(A) Transmission electron microscopy (TEM) images of the middle-distal part of a comb plate showing aligned orientation of ciliary axonemes in the control larva (left) and those including cilia with the plane of central pair microtubules out of alignment in the CTENO64 morphant larva (right; MO1). The orientations of axonemes are indicated by the direction from doublet 8 to 3 (red arrows). The direction of the comb plate effective stroke is indicated on the left; oral (o) to aboral (a) side of the larva. Axonemes lacking one or all compartmenting lamellae (CL) are indicated in pink. Cilia with inverted orientation of the axonemes are indicated in blue. Bar, 200 nm. (B) Circular histograms showing the orientation of axonemes in the control (left) and CTENO64 morphant larvae (right; MO1) comb plates. The red bar represents the angle range (counted for every 20°) between the central axis of the central pair microtubule and the direction of effective stroke. n = 409 (control); 544 (MO1).

2.4 Discussion

Ctenophore comb plate is a large assembly of numerous cilia and can be several millimeters in width and length. The CLs that connect each cilium are thought to be essential for the construction and coordinated movement of a comb plate. Here, I first identified a protein component of CL, CTENO64, which was localized in the proximal part of a comb plate and was essential for the formation of CL. CTENO64 deficiency causes a loss of CL; however, neither ciliary formation nor the basic properties of ciliary beating, such as beat frequency, were affected. The most striking finding was the disorientation of ciliary axonemes in the CTENO64 morphant larvae. The plane of the central pair of microtubules in cilia lacking CL became out of alignment with those with CL. This would possibly lead to non-planar and three-dimensional beating of comb plates in the CTENO64 morphant larvae.

The knockdown of CTENO64 caused a loss of CL structures not only in the proximal region but also throughout the comb plate, suggesting that CTENO64 might act as a scaffold to construct whole CL. Macrocilia of *Beroe* are formed in two patterns, one of which accompanies a stump-like base at the proximal end of the macrocilia. Ciliogenesis occurs from the oral side of macrocilia (Tamm and Tamm, 1988). Therefore, CTENO64 is possibly involved in the construction of the first base for the formation of a comb plate, similar to the stump in the ciliogenesis of macrocilia, being located in the vicinity of doublet microtubules and specifically connecting CL to doublets 3 and 8. In this case, the CL in the middle and distal regions would be formed on the basis of CTENO64-based scaffold CL, since no CL were observed around these regions in the morphant larvae.

The orientation of the ciliary axonemes is aligned during the development of epithelial monocilia in sea urchins (Mizuno et al., 2017) and multicilia in *Xenopus* (Mitchell et al., 2007) by hydrodynamic feedback from ciliary beating. However, structural loss at the base of a cilium (Kinoshita and Murakami, 2012) or an aberrant bend propagation (Mizuno et al., 2017) results in failure of the orientation establishment, suggesting that proper generation of fluid flow is essential for hydrodynamic feedback. In the CTENO64 morphant larvae, 46.7% of ciliary axonemes were not oriented at 30 hpf, by which almost all cilia in the control comb plates had already been aligned and properly beaten. Some CL-deficient cilia in the morphant comb plates had the same orientation as those of CL-bearing normal cilia, suggesting the remediation of ciliary alignment through hydrodynamic force. However, the cilia with caracole orientations were perpendicularly aligned in the middle to distal region of a comb plate. Therefore, it seems that ciliary alignment is not always

remediated by hydrodynamic force, but this would be primarily determined by CTENO64-mediated scaffolding at the base of a comb plate.

In addition to the regulation of axonemal orientation, hydrodynamic feedback also regulates the coordination of movement for efficient production of surface fluid flow, a process known as metachronal wave propagation (Kinoshita and Hirano, 1967; Machemer, 1972). Comb plates along a comb row coordinate their beating to generate metachronal waves for effective propulsion (Horridge, 1965; Sleigh, 1963; Tamm, 1973; Tamm, 1984). In CTENO64 morphant larvae, some comb plates exhibit three-dimensional beating due to the inclusion of non-aligned axonemes; however, metachronal propagation of comb plate beating is not perturbed. The metachronal waves along a comb row are thought to be induced by two mechanisms: mechanical transmission through structures called interplate ciliated grooves (ICGs) (Tamm, 1973; Tamm, 2014) in Lobata, and hydromechanical coupling between comb plates in other ctenophores (Tamm, 1984; Tamm, 2014). ICGs adjoin the comb plates but do not run through them internally (Tamm, 2014). Therefore, it is likely that the change in beating observed in CTENO64 morphant larvae does not affect the function of ICGs in terms of the mechanical transmission from one comb plate beating to an adjacent one. A knockdown experiment of the CTENO64 orthologs in non-Lobata species would be informative to conclude whether CLs are essential for the hydrodynamic propulsion of successive metachronal coordination in comb plate beating.

The Reynolds number (Re) of a motile system determines the flow in an aquatic solution. It is affected by the length and angular velocity of a substance. If it is less than one, such as a case with low velocity or smaller size, then the viscous forces become dominant, as seen in sperm and protists, while if the value is more than one, then inertial forces dominate the viscous forces (Blake and Sleigh, 1974; Barlow and Sleigh, 1993; Matsumoto, 1991). Therefore, comb plate movements in ctenophores should have a large Re and be highly affected by inertial force. For example, in *Pleurobrachia pileus* the Re was 9 when calculated for a 0.8 mm comb plate beating at 10 Hz (Barlow and Sleigh, 1993). The comb plate is an exceptionally large size for ciliary forms among organisms and would receive such mechanical stresses that are not seen in any smaller ciliary forms, and as such would induce interciliary space flow (Matsumoto, 1991). A part of cilia in the CTENO64-deficient comb plate showed caracole orientation at the distal end. However, their orientation changed to perpendicular at the middle to distal end, suggesting a possibility that these cilia are twisted over the entire length of a comb plate. This might be also caused by the mechanical stresses.

The signals of western blot and immunofluorescence mostly disappeared in the CTENO64 morphant larvae (Fig. 2.10, 2.11A), indicating that CTENO64 was successfully knocked down. However, the effect was only partial because only ~16% of the cilia in the comb plate lacked CL. This suggests that the role of CTENO64 in the formation of CL might be compensated by other components of CL. Identification of other proteins component in CL would be the next step toward understanding the structure-function relationship of CL.

Chapter 4

Conclusion and Perspective

In this thesis, I identified the novel proteins CTENO64 and CTENO189 as components of the compartmenting lamellae (CL) of the comb plates in ctenophores. The knockdown of *CTENO64* caused loss of CL in partial, but rather the orientation of axonemes was greatly disturbed. This result suggests that CTENO64 is an important factor in determining the ciliary orientation in the comb plate. CTENO64 was also found to be involved in normal propagation of bending. In contrast, the knockdown of *CTENO189* caused a significant loss of the dCL in the comb plates but did not affect the axonemal orientation. This result suggests that CTENO189 functions as the core scaffold protein for the dCL formation. CTENO189 is also important for maintaining the asymmetrical waveforms of the comb plate beating and is involved in the formation of normal metachronal waves. However, these CL proteins were completely separated in the comb plates; proximal and distal regions for CTENO64 and CTENO189, respectively. Clear differences in the components suggest that the functions are quite different in these CL regions. In other words, these findings provide a new insight that CL is not only the structural links between cilia but also plays important roles in the regulation for efficient ciliary movement of the giant compound cilia, comb plate (Fig. 4.1).

The cilia were originally functional under a microfluid world at a low Reynolds number where viscosity resistance dominates, so that the organisms that use cilia for swimming are small in size. The relative speed generated by ciliary movement is about ten times the body length per second (Blake and Sleigh, 1974; Matsumoto, 1991). However, ctenophores are in very large size, and the comb plates receive ten times more inertial resistance than viscous resistance (Barlow et al., 1993). In fact, the comb plates are thought to move under high Re, estimated as 10-300. In order to overcome this condition, it is considered that ctenophores convergently acquired the CL during the process of enlarging compound cilia. The comb plates are thought to cooperatively capture the accelerated backflow produced around other comb plates (Barlow et al.,1993; Barlow and Sleigh, 1993), which is seemingly a unique mechanism acquired in high Re world.

In general, when cilia are arranged in a row, each cilium has hydrodynamic interaction between adjacent cilium, forming a metachronal wave with a constant phase difference (Sleigh, 1963). Antiplectic metachronal waves are suitable for fast delivery of low-viscosity liquids because the distance between the cilia becomes longer during effective stroke (Knight-Jones, 1954). In addition, the antiplectic metachronal waves is considered to form a more efficient flow in an environment affected by inertia. Under mathematical model conditions where inertial effects occur, asymmetric ciliary waveforms play an important role in maintaining antiplectic metachronal waves (Hussong et

al., 2011). In CTENO189 morphant larvae, the asymmetric movements of the comb plate movements were disturbed and further the phase difference between adjacent comb plates remarkably decreased, resulting in the loss of metachronous rhythm. Therefore, the asymmetric waveforms generated by the help of CTENO189 in the dCL would be important for the maintaining of antiplectic metachronal waves and ultimately be necessary for the ctenophore to swim in high Re fluid condition.

Both CTENO64 and CTENO189 are the components of one of the ctenophore-specific characteristics, CLs. The idea that "primitive" living species are ancestors of "complex" living species was widespread, even though the complex characteristics acquired in various species could be reduced or lost. Recent phylogenomic view of the ctenophores demonstrates only the resultant characteristics through evolution in bilaterian biology, although all organisms might have a mix of shared characteristics, including unique ones, with other organisms (Dunn et al., 2015). Thus, there may be many aspects of "hidden biology" that have not been discovered yet. The finding of two CL proteins in this study is an example of "hidden biology" that directs to explore a unique characteristic in the ctenophores. However, it should also shed light on new connections with other organisms and unique evolutionary pathways of these animals.

Since all the cilia in a comb plate are regularly arranged with almost same direction, the comb plates have a crystalline property and emit a structural color (Welch et al., 2005). The evolution of structural colors is thought to have initiated in the Cambrian explosion (Parker, 2005). In fact, fossils of the ctenophores with comb plates were recently discovered in the Cambrian period (e.g. Zhao et al., 2019). The structural colors are one of the important communication tools between animals such as camouflage and courtship. Therefore, in addition to the point of view for hydrodynamic preference, the structural basis of the comb plate may provide important insights into another biological significance of the comb plates, *i.e*. how their acquisition have brought about ecological benefits in the ctenophores. Finally, the crystalline properties of comb plates might provide a powerful biological material for structural biology. Bundling of numerous numbers of the axonemes with CL components *in vitro* may lead to the formation of a giant crystal of axonemes, which not only make it possible to determine the axonemal structure at subnanometer level by X-ray diffraction, but also lead to the development of "motile" photonic crystals, which would exploit a new technology in photonics.

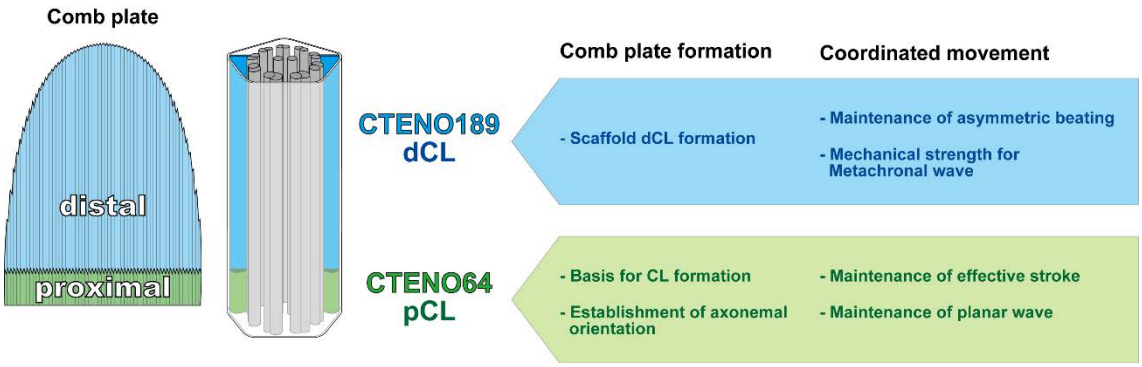

Figure 4.1. Two compartments of comb plates and their components and the function in motility
Molecular and functional separation of the comb plate into two compartments is one of the major conclusions in this thesis. The connecting structure between comb plate cilia, the compartmenting lamella (CL), is structurally and functionally different between proximal and distal regions. Proximal CL (pCL) and distal CL (dCL) contain different components, CTENO64 and CTENO189, respectively, and play distinct roles in the formation and coordinated movement of the comb plates (also see Discussion, Chapter 3).

Reference

Afzelius, B. A. (1961). The fine structure of cilia from ctenophore swimming plates. *J. Biophys. Biochem. Cytol.* 9, 383-394.

Babonis, L. S., DeBiasse, M. B., Francis, W. R., Christianson, L. M., Moss, A. G., Haddock, S. H., Martindale, M. Q., and Ryan, J. F. (2018). Integrating embryonic development and evolutionary history to characterize tentacle-specific cell types in a ctenophore. *Mol. Biol. Evol.* 35, 2940-2956.

Barlow, D., Sleigh, M. A., and White, R. J. (1993). Water flows around the comb plates of the ctenophore *Pleurobrachia* plotted by computer: A model system for studying propulsion by antipleitic metachronism. *J. Exp. Biol.* 177, 113-128.

Barlow, D., and Sleigh, M. A. (1993). Water propulsion speeds and power output by comb plates of the ctenophore *Pleurobrachia pileus* under different conditions. *J. Exp. Biol.* 183, 149-164.

Blake, J. R., and Sleigh, M. A. (1974). Mechanics of ciliary locomotion. *Biol. Rev.* 49, 85-125.

Chun, C. (1880). Die Ctenophoren des Golfes von Neapel. *Fauna Flora Golfes Neapel* 1, 1-311.

Colin, S. P., Costello, J. H., Hansson, L. J., Titelman, J., and Dabiri, J. O. (2010). Stealth predation and the predatory success of the invasive ctenophore *Mnemiopsis leidyi*. *Proc. Natl. Acad. Sci. U.S.A.* 107, 17223-17227.

Dentler, W. L. (1981). Microtubule-membrane interactions in cilia and flagella. *Int. Rev. Cytol.* 72, 1-47.

Driesch, H., and Morgan, T. H. (1895). Zur Analysis der ersten Entwickelungsstadien des Ctenophoreneies. *Archiv für Mikroskopische Anatomie* 2, 204-215.

Dunn, C. W., Hejnol, A., Matus, D. Q., Pang, K., Browne, W. E., Smith, S. A., Seaver, E., Rouse, G. W., Obst, M., Edgecombe, G. D., Sørensen, M. V., Haddock, S. H., Schmidt-Rhaesa, A., Okusu, A., Kristensen, R. M., Wheeler, W. C., Martindale, M. Q., and Giribet, G. (2008). Broad phylogenomic sampling improves resolution of the animal tree of life. *Nature* 452, 745-749.

Dunn, C. W., Leys, S. P., and Haddock, S. H. (2015). The hidden biology of sponges and ctenophores. *Trends Ecol. Evol.* 30, 282-291.

Elgeti, J., and Gompper, G. (2013). Emergence of metachronal waves in cilia arrays. *Proc. Natl. Acad. Sci. U.S.A.* 110, 4470-4475.

Franc, J. M. (1978). Organization and function of ctenophore colloblasts: an ultrastructural study. *Biol. Bull.* 155, 527-541.

Gibbons, I. R., and Fronk, E. (1972). Some properties of bound and soluble dynein from sea urchin sperm flagella. *J. Cell Biol.* 54, 365-381.

Granhag, L., Majaneva, S., and Moller, L. F. (2012). First recordings of the ctenophore *Euplokamis* sp (Ctenophora, Cydippida) in Swedish coastal waters and molecular identification of this genus. *Aquat. Invasions* 7, 455-463.

Gray, J. (1930). The mechanism of ciliary movement.—VI. Photographic and stroboscopic analysis of ciliary movement. *Proc. Royal Soc. B* 107, 313-332.

Hernandez-Nicaise, M. L. (1973). The nervous system of ctenophores III. Ultrastructure of synapses. *J. Neurocytol.* 2, 249-263.

Hirano, M., and Hirano, T. (2002). Hinge-mediated dimerization of SMC protein is essential for its dynamic interaction with DNA. *EMBO J.* 21, 5733-5744.

Horridge, G. A. (1964). The giant mitochondria of ctenophore comb plates. *Q. J. Microsc. Sci.* 105, 301-310.

Horridge, G. A. (1965). Intracellular action potentials associated with the beating of the cilia in ctenophore comb plate cells. *Nature* 205, 602.

Horridge, G. A. (1974). Recent studies on the Ctenophora. In: *Coelenterate Biology,* Muscatine, L., and Lenhoff, H. M. (eds.), Academic Press, New York, pp. 439-468.

Hussong, J., Breugem, W. P., and Westerweel, J. (2011). A continuum model for flow induced by metachronal coordination between beating cilia. *J. Fluid Mech.* 684, 137-162.

Inaba, K., Mohri, T., and Mohri, H. (1988). B-band protein in sea urchin sperm flagella. *Cell Motil. Cytoskeleton* 10, 506-517.

Jager, M., Chiori, R., Alié, A., Dayraud, C., Quéinnec, E., and Manuel, M. (2011). New insights on ctenophore neural anatomy: immunofluorescence study in *Pleurobrachia pileus* (Müller, 1776). *J. Exp. Zool. B* 316, 171-187.

Jokura, K., Shibata, D., Yamaguchi, K., Shiba, K., Makino, Y., Shigenobu, S., and Inaba, K. (2019). CTENO64 is required for coordinated paddling of ciliary comb plate in ctenophores. *Curr. Biol.* 29, 3510-3516.

Kinoshita, H., and Murakami, A. (1967). Control of ciliary motion. *Physiol. Rev.* 47, 53-81.

Knight-Jones, E. W. (1954). Relations between metachronism and the direction of ciliary beat in Metazoa. *J. Cell Sci.* 3, 503-521.

Leys, S. P. (2019). Animal evolution: The hidden biology of the ctenophore cilium. *Curr. Biol.* 29, 1079-1081.

Lim, D., Lahooti, M., and Kim, D. (2019). Inertia-driven flow symmetry breaking by oscillating plates. *AIP Adv.* 9, 105119.

Linck, R. W., Stephens, R. E., and Tamm, S. L. (1991). Evidence for tektins in cilia from the ctenophore, *Mnemiopsis leidyi.* In: *Comparative spermatology 20 years after*, Baccetti, B. (ed.), Raven Press, New York, pp. 391-395.

Machemer, H. (1972). Ciliary activity and the origin of metachrony in *Paramecium*: Effects of increased viscosity. *J. Exp. Biol.* 57, 239-259.

Mackie, G. O., Mills, C. E., and Singla, C. L. (1988). Structure and function of the prehensile tentilla of *Euplokamis* (Ctenophora, Cydippida). *Zoomorphology* 107, 319-337.

Markova, S. V., Burakova, L. P., Golz, S., Malikova, N. P., Frank, L. A., and Vysotski, E. S. (2012). The light-sensitive photoprotein berovin from the bioluminescent ctenophore *Beroe abyssicola*: a novel type of Ca^{2+}-regulated photoprotein. *FEBS J.* 279, 856-870.

Martindale, M. Q. (1986). The ontogeny and maintenance of adult symmetry properties in the ctenophore, *Mnemiopsis mccradyi*. *Dev. Biol.* 118, 556-576.

Martindale, M. Q., and Henry, J. Q. (1995). Diagonal development: establishment of the anal axis in the ctenophore *Mnemiopsis leidyi*. *Biol. Bull.* 189, 190-192.

Martindale, M. Q., and Henry, J. Q. (1997). Reassessing embryogenesis in the Ctenophora: the inductive role of e1 micromeres in organizing ctene row formation in the 'mosaic' embryo, *Mnemiopsis leidyi*. *Development* 124, 1999-2006.

Martindale, M. Q., and Henry, J. Q. (1999). Intracellular fate mapping in a basal metazoan, the ctenophore *Mnemiopsis leidyi*, reveals the origins of mesoderm and the existence of indeterminate cell lineages. *Dev. Biol.* 214, 243-257.

Martindale, M. Q., and Henry, J. Q. (2015). Ctenophora. In: *Evolutionary Developmental Biology of Invertebrates 1*, Wanninger A. (ed.), Springer, Vienna, pp. 179-201

Matsumoto, G. I. (1991). Swimming movements of ctenophores, and the mechanics of propulsion by ctene rows. *Hydrobiologia* 216, 319-325.

Maxwell, E. K., Ryan, J. F., Schnitzler, C. E., Browne, W. E., and Baxevanis, A. D. (2012). MicroRNAs and essential components of the microRNA processing machinery are not encoded in the genome of the ctenophore *Mnemiopsis leidyi*. *BMC Genom.* 13, 714.

Mitchell, B., Jacobs, R., Li, J., Chien, S., and Kintner, C. (2007). A positive feedback mechanism governs the polarity and motion of motile cilia. *Nature* 447, 97-101.

Mizuno, K., Shiba, K., Yaguchi, J., Shibata, D., Yaguchi, S., Prulière, G., Chenevert, J., and Inaba, K. (2017). Calaxin establishes basal body orientation and coordinates movement of monocilia in sea urchin embryos. *Sci. Rep.* 7, 10751.

Moroz, L. L., Kocot, K. M., Citarella, M. R., Dosung, S., Norekian, T. P., Povolotskaya, I. S., Grigorenko, A. P., Dailey, C., Berezikov, E., Buckley, K. M., *et al.* Ptitsyn, A., Reshetov, D., Mukherjee, K., Moroz, T. P., Bobkova, Y., Yu, F., Kapitonov, V. V., Jurka, J., Bobkov, Y. V., Swore, J. J., Girardo, D. O., Fodor, A., Gusev, F., Sanford, R., Bruders, R., Kittler, E., Mills, C. E., Rast, J. P., Derelle, R., Solovyev, V. V., Kondrashov, F. A., Swalla, B. J., Sweedler, J. V., Rogaev, E. I., Halanych, K. M., and Kohn, A. B. (2014). The ctenophore genome and the evolutionary origins of neural systems. *Nature* 510, 109-114.

Nakachi, M., Nakajima, A., Nomura, M., Yonezawa, K., Ueno, K., Endo, T., and Inaba, K. (2011). Proteomic profiling reveals compartment-specific, novel functions of ascidian sperm proteins. *Mol. Reprod. Dev.* 78, 529-549.

Nakamura, S., and Tamm, S. L. (1985). Calcium control of ciliary reversal in ionophore-treated and

ATP-reactivated comb plates of ctenophores. *J. Cell Biol.* 100, 1447-1454.

Neff, E. P. (2018). What is a lab animal?. *Lab Anim*. 47, 223.

Omoto, C. K., and Kung, C. (1979). The pair of central tubules rotates during ciliary beat in Paramecium. *Nature* 279, 532-534.

Padma, P., Satouh, Y., Wakabayashi, K. I., Hozumi, A., Ushimaru, Y., Kamiya, R., and Inaba, K. (2003). Identification of a novel leucine-rich repeat protein as a component of flagellar radial spoke in the ascidian *Ciona intestinalis*. *Mol. Biol. Cell* 14, 774-785.

Pang, K., and Martindale, M. Q. (2008). Ctenophore whole-mount antibody staining. *Cold Spring Harb. Protoc.*11, 5086.

Parker, A. R. (2005). A geological history of reflecting optics. *J. Royal Soc. Interface* 2, 1-17.

Porter, M. E., and Sale, W. S. (2000). The 9+2 axoneme anchors multiple inner arm dyneins and a network of kinases and phosphatases that control motility. *J. Cell Biol.* 151, 37-42.

Ryan, J. F., Pang, K., Schnitzler, C. E., Nguyen, A. D., Moreland, R. T., Simmons, D. K., Koch, B. J., Francis, W. R., Havlak, P., NISC Comparative Sequencing Program, Smith, S. A., Putnam, N. H., Haddock, S. H., Dunn, C. W., Wolfsberg, T. G., Mullikin, J. C., Martindale, M. Q., and Baxevanis, A. D. (2013). The genome of the ctenophore *Mnemiopsis leidyi* and its implications for cell type evolution. *Science* 342, 1242592.

Sasson, D. A., Jacquez, A. A., and Ryan, J. F. (2018). The ctenophore *Mnemiopsis leidyi* regulates egg production via conspecific communication. *BMC Ecol.* 18, 12.

Sebé-Pedrós, A., Chomsky, E., Pang, K., Lara-Astiaso, D., Gaiti, F., Mukamel, Z., Amit, I., Hejnol, A., Degnan, B. M., and Tanay, A. (2018). Early metazoan cell type diversity and the evolution of multicellular gene regulation. *Nat. Ecol. Evol.* 2, 1176-1188.

Shiba, K., Baba, S. A., Inoue, T., and Yoshida, M. (2008). Ca^{2+} bursts occur around a local minimal concentration of attractant and trigger sperm chemotactic response. *Proc. Natl. Acad. Sci. U.S.A.* 105, 19312-19317.

Simion, P., Bekkouche, N., Jager, M., Queinnec, E., and Manuel, M. (2015). Exploring the potential of small RNA subunit and ITS sequences for resolving phylogenetic relationships within the phylum Ctenophora. *Zoology* 118, 102-114.

Sleigh, M. A. (1962). In: *The Biology of Cilia and Flagella*, Sleigh M. A. (ed.), Pergamon Press, Oxford.

Sleigh, M. A. (1963). Movements and co-ordination of the ciliary comb plates of the ctenophores *Beroe* and *Pleurobrachia*. *Nature* 199, 620-621.

Stephens, R. E. (1970). Thermal fractionation of outer fiber doublet microtubules into A- and B-subfiber components: A- and B-tubulin. *J. Mol. Biol.* 47, 353-363.

Tamm, S. L. (1973). Mechanisms of ciliary coordination in ctenophores. *J. Exp. Biol.* 59, 231-245.

Tamm, S. L. (1982). Ctenophora. In: *Electrical conduction and behavior in "simple" invertebrates*,

Shelton, G. A. B. (ed.), Clarendon Press, Oxford, pp. 266-358.

Tamm, S. L. (1983). Motility and mechanosensitivity of macrocilia in the ctenophore *Beroë*. *Nature* 305, 430-433.

Tamm, S. L. (1984). Mechanical synchronization of ciliary beating within comb plates of ctenophores. *J. Exp. Biol.* 113, 401-408.

Tamm, S. L. (2012). Patterns of comb row development in young and adult stages of the ctenophores *Mnemiopsis leidyi* and *Pleurobrachia pileus*. *J. Morphol.* 273, 1050-1063.

Tamm, S. L. (2014). Cilia and the life of ctenophores. *Invertebr. Biol.* 133, 1-46.

Tamm, S. L. (2019). Defecation by the ctenophore *Mnemiopsis leidyi* occurs with an ultradian rhythm through a single transient anal pore. *Invertebr. Biol.* 138, 3-16.

Tamm, S. L., and Moss, A. G. (1985). Unilateral ciliary reversal and motor responses during prey capture by the ctenophore *Pleurobrachia*. *J. Exp. Biol.* 114, 443-461.

Tamm, S. L., and Tamm, S. (1981). Ciliary reversal without rotation of axonemal structures in ctenophore comb plates. *J. Cell Biol.* 89, 495-509.

Tamm, S. L., and Tamm, S. (1984). Alternate patterns of doublet microtubule sliding in ATP-disintegrated macrocilia of the ctenophore *Beroë*. *J. Cell Biol.* 99, 1364-1371.

Tamm, S. L., and Tamm, S. (1985). Visualization of changes in ciliary tip configuration caused by sliding displacement of microtubules in macrocilia of the ctenophore *Beroe*. *J. Cell Sci.* 79, 161-179.

Tamm, S., and Tamm, S. L. (1988). Development of macrociliary cells in *Beroe*. II. Formation of macrocilia. *J. Cell Sci.* 89, 81-95.

Weill, R. (1935). Structure, origine et interpretation cytologiquedes colloblastes de *Lampetia pancerina*. *Comptes Rendus Acad. Sci.* 200, 1628-1630.

Welch, V. L., Vigneron, J. P., and Parker, A. R. (2005). The cause of colouration in the ctenophore *Beroe cucumis*. *Curr. Biol.* 15, 985-986.

Whelan, N. V., Kocot, K. M., Moroz, T. P., Mukherjee, K., Williams, P., Paulay, G., Moroz, L. L., and Halanych, K. M. (2017). Ctenophore relationships and their placement as the sister group to all other animals. *Nat. Ecol. Evol.* 1, 1737-1746.

Yagi, T., Uematsu, K., Liu, Z., and Kamiya, R. (2009). Identification of dyneins that localize exclusively to the proximal portion of *Chlamydomonas* flagella. *J. Cell Sci.* 122, 1306-1314.

Yamada, A., Martindale, M. Q., Fukui, A., and Tochinai, S. (2010). Highly conserved functions of the Brachyury gene on morphogenetic movements: insight from the early-diverging phylum Ctenophora. *Dev. Biol.* 339, 212-222.

Zhao, Y., Vinther, J., Parry, L. A., Wei, F., Green, E., Pisani, D., Hou, X., Edgecombe, G. D., and Cong, P. (2019). Cambrian sessile, suspension feeding stem-group ctenophores and evolution of the comb jelly body plan. *Curr. Biol.* 29, 1112-1125.

Acknowledgment

I would like to show my greatest appreciation to my supervisor Professor Kazuo Inaba for his generous support and invaluable advice throughout the course of this study. I would like to express the deepest appreciation to Dr. Kogiku Shiba for her technical guidance and encouragement. I am deeply grateful to Dr. Daisuke Shibata for his technical supports. Without his hard guidance for rearing the comb jellies used for experiment, this study would not have materialized. I want to thank Ms. Masae Ohata and Ms. Tomomi Kodaka for their help for rearing the comb jellies. I am deeply grateful to technical staffs of Shimoda Marine Research Center, Hisanori Kohtsuka and Michiyo Kawabata (Misaki Marine Biological Station), Shinichiro Ikeguchi, Naoya Hirata, and Momoka Nagai (Notojima Aquarium), So Abe and Michikazu Yorozu (Hakkeijima Sea Paradise) for their support of collecting comb jellies. I would like to express my gratitude to Dr. Atsuo Nishino for his suggestions about injection techniques, Dr. Ben Harvey for his advice about English grammar and Dr. Naoki Noda for his encouragement. Finally, I thank my family for their encouragement.